Manufacturing Rev. **10**, 2 (2023)

https://doi.org/10.1051/mfreview/2022035

Manufacturing Review
Available online at:
https://mfr.edp-open.org

REVIEW OPEN ACCESS

Topological structures for microchannel heat sink applications – a review

Kaijie Lu[1], Chunju Wang[1,*], Changrui Wang[2], Xueliang Fan[3], Fei Qi[1] and Haidong He[1]

[1] School of Mechanical and Electrical Engineering, Robotics and Microsystems Center, Soochow University, Suzhou 215131, China
[2] School of Mechanical and Electrical Engineering, Nanjing University of Aeronautics and Astronautics, Nanjing 210016, China
[3] School of Rail Transportation, Soochow University, Suzhou 215131, China

Received: 2 October 2022 / Accepted: 22 November 2022

Abstract. The microchannel heat sink (MCHS) has the advantages of small heat transfer resistance, high heat transfer efficiency and small size, which exhibits good heat transfer performance in the field of active heat dissipation of electronic devices integrated with high heat flux density. In this paper, the application of MCHS in thermal management is reviewed in recent years, and the research progress of microchannel topology on enhancing heat transfer performance is summarized. Firstly, the research progress on the cross-sectional shape of the microchannel shows that the heat transfer area and fluid flow dead zone of the microchannel is the keys to affecting the heat transfer performance; Secondly, the microchannel distribution and the bionic microchannel structure have a great role in enhancing heat transfer performance, especially in microchannel temperature uniformity; Thirdly, the disturbing effect caused by interrupted structures in microchannels such as ribs and concave cavities has become a hot topic of research because it can weaken the thermal boundary layer and increase heat dissipation. Finally, the commonly used MCHS materials and cooling media are summarized and introduced. Based on the above reviews of MCHS research and applications, the future trends of MCHS topologies are presented.

Keywords: Microchannel heat sink / bionic structure / fluid interruption / thermally conductive material / cooling fluid

1 Introduction

In recent years, with the rapid development of integrated devices such as chips toward a high degree of miniaturization and intelligence, especially in the field of military applications, the heat flow per unit area generated by the operation of integrated devices will reach an unprecedented height. According to the International Technology Roadmap for Semiconductors (ITRS), the heat flux density of future integrated devices will reach 1000 W/cm^2 [1]. The problem of high heat flow density can reduce the performance of the equipment, which seriously affects the safety and reliability of the integrated equipment or even damage it. According to statistics, for every 10 °C increase in the operating temperature of electronic components, the failure rate will increase exponentially, and the system reliability will be reduced by 50% accordingly, while 80% of chip failures are due to high temperatures. In addition, Black's equation [2] indicated that the temperature problem is the main reason for the failure of electronic devices. The first- and second-generation core chips use high thermal conductivity management materials and liquid-cooled heat dissipation combinations that can no longer meet the current heat dissipation needs, and it is urgent to find efficient heat dissipation and cooling technologies [3]. In the 1980 s, Tuckerman and Pease [4] compared the heat dissipation performance of MCHS with that of conventional finned devices and showed that the heat sink structure in MCHS significantly improved heat transfer efficiency. In recent years, MCHS has been widely used in heat dissipation applications for high heat flux integrated devices in the fields of aviation, radar and new energy due to their small size, good heat transfer performance and light weight.

Compared with traditional large-channel heat sinks, MCHS has higher heat transfer efficiency because of their larger heat transfer surface area-to-volume ratio and lower heat transfer temperature difference. In addition, there are many factors that affect the heat dissipation performance of the MCHS, including the design of the microchannel heat sink structure, the selection of the microchannel heat sink

* e-mail: cjwang@suda.edu.cn

material, and the characteristics of the medium fluid. When designing a MCHS, these influencing factors need to be comprehensively considered. The heat transfer performance of MCHS is often limited by the difficulty and high cost of heat sink structure fabrication, the poor thermal conductivity of heat sink materials, fluid energy loss, and large fluid temperature gradients. In addition, the uneven temperature distribution of the device caused by the uneven flow distribution of the microchannel will also reduce the equipment reliability of the integrated device [5].

In the past two or three decades since the study of microchannel radiators, most studies have focused on solid parallel microchannels, of which the most common is the rectangular microchannel structure. However, in view of the heat dissipation requirements of practical applications in the aerospace field, the traditional rectangular parallel microchannels have been unable to meet the thermal management of high heat flux devices. Therefore, to improve the heat transfer performance of the MCHS, researchers have taken a lot of work on the structural design of the MCHS, mainly including the design of the special-shaped cross-sectional channels, the bionic topology design of the MCHS and the fluid interruption structure design. Among them, the replacement of rectangular cross-sectional structures by triangular or trapezoidal cross-sectional structures is the most widely used in the design of microchannel structures with special-shaped cross-sections. The significance of the biomimetic topology design is to improve the disturbance of the fluid in the channel and reduce the temperature difference by learning from the biological advantages of its own structure. In addition, high aspect ratio microchannels with rib and cavity structures, which increase the heat transfer area while promoting fluid disturbance, have also become the predominant solution for enhanced heat transfer performance. These structural designs have been shown to be very effective in enhancing the heat dissipation performance of microchannels. In addition, active heat transfer mainly includes single-phase flow heat transfer and two-phase flow heat transfer, and boiling heat transfer is the most common one in two-phase heat transfer. The rib and cavity structure can not only increase the number of nucleation points of boiling bubbles in the boiling heat transfer but also effectively prevent the wall surface from drying due to the boiling heat transfer.

The choice of heat sink material also plays a crucial role in enhancing the heat transfer performance of the microchannels. The previous heat dissipation materials for electronic packaging have low thermal conductivity or high thermal expansion coefficient, which cannot meet the application requirements. Metal matrix composites have good thermal conductivity, tunable expansion coefficient and low density, which have been the hotspot of research and application in recent years. In addition, due to the different specific heats of different fluid media, the ability to transfer device heat and reduce device temperature in convective heat transfer is different. Therefore, the selection of the fluid medium is also extremely important for the improvement of the heat transfer performance of the microchannel.

The summary of this review is under the trend of the era of rapid development of high heat flux density electronic device integration. To improve the temperature reliability of integrated devices in aerospace and microelectronics, the design and manufacture of MCHS to achieve forced convection heat transfer and reduce device temperature has become the focus of research into the temperature control of integrated devices. This review analyses and discusses the research progress in the past few years on the design of MCHS structures to reduce the operating temperature of high heat flow density electronic devices. In particular, the heat transfer and fluid performance of heat sinks under different geometrical designs including shaped cross-sectional channel designs, topological bionic structure designs and fluid disruption structure designs. The article also discusses and prospects the selection of MCHS materials and the types of fluid media in recent years. This review has certain reference significance for the development and application of high-performance microchannel heat sinks and the design of channel structures.

2 Single-phase flow microchannel structure optimization

The geometric design of the microchannel plays a crucial role in enhancing the heat transfer performance of the MCHS. It can not only increase the actual heat exchange area of the heat sink but also change the flow mode of the fluid and improve the uniformity of the flow distribution. The geometric structure design of the microchannel includes the design of the special-shaped cross-section channel, the design of the bionic topology and the structure design of the cavity and the reinforcing rib in the channel. Microchannel geometry design improves heat transfer mechanisms by reducing thermal boundary layer thickness, promoting fluid mixing, and enhancing fluid velocity gradients across heated surfaces [6].

2.1 Special-shaped cross-section channel

The cross-sectional shape of the microchannel has a significant effect on increasing the heat transfer area and improving the flow behavior of the cooling medium, which determines the heat transfer performance. A great deal of research has been carried out by domestic and international scholars on the effect of section shape on heat transfer performance. As early as 1998, Perret et al. [7] proposed forming microchannels on silicon substrates as a forced liquid cooling device for integrated circuits and analyzed the heat dissipation characteristics of three cross-sectional shapes including rectangular, rhombic and hexagonal microchannels by numerical simulations and theoretical calculations. The rectangular cross-section microchannel exhibits the lowest heat transfer thermal resistance. Wu and Cheng [8] used the same method to fabricate trapezoidal and triangular cross-section microchannels and compared the heat dissipation performance of trapezoidal silicon microchannels with 13 different surface roughness and channel geometry parameters. It was found that the effect of section geometry parameters on the heat transfer performance is much greater than the effect of surface roughness. Therefore, the investigation of cross-sectional geometrical parameters is of great significance for the heat transfer performance of

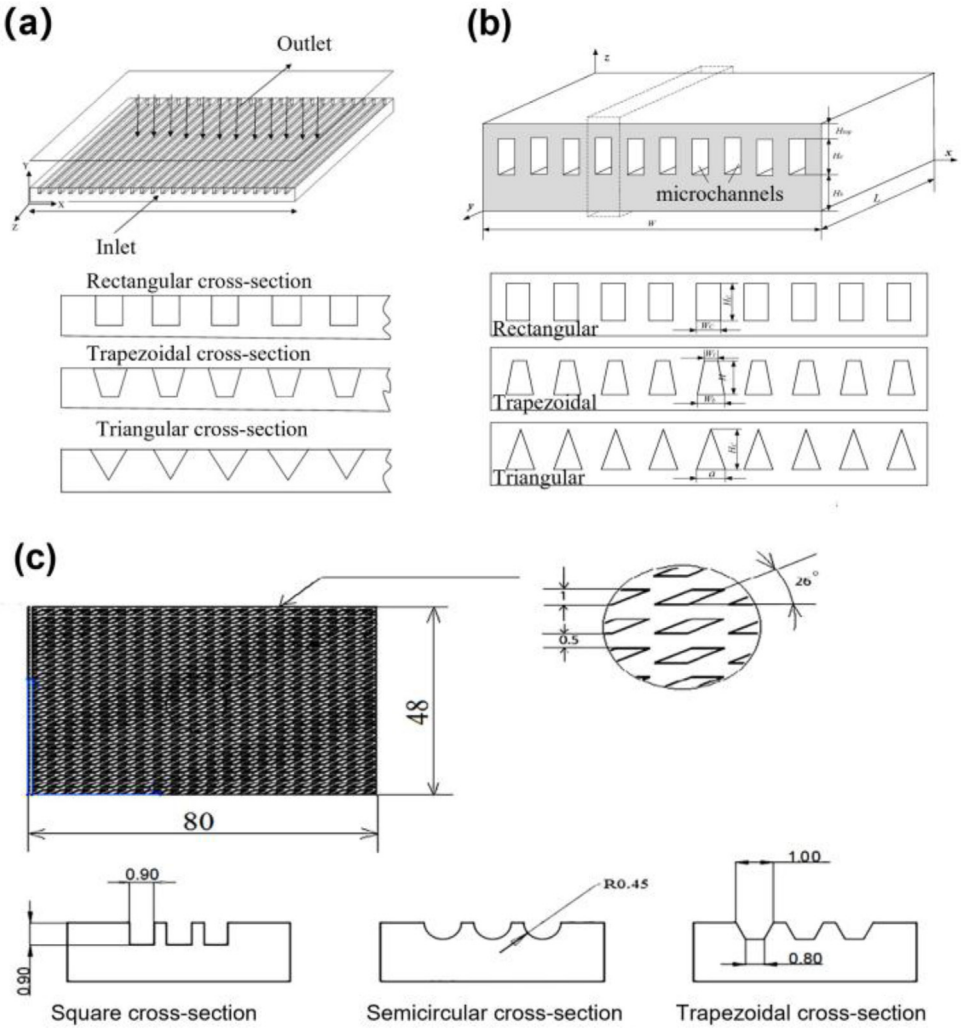

Fig. 1. Different cross-sectional shapes of microchannels (a) Rectangular, trapezoidal and triangular cross-sections [10] (b) Rectangular, trapezoidal and triangular cross-sections [11] (c) Rectangular, semicircular and trapezoidal cross-sections [12].

channels. Chen et al. [9] etched parallel microchannels with rectangular, triangular, and trapezoidal cross-sectional shapes on silicon wafers and compared their required pumping power and heat transfer efficiency with the variation of different Reynolds numbers (Re), in which the triangular microchannel requires the least pumping power and has the highest thermal efficiency. Gunnasegaran and Wang [10,11] showed that the heat transfer characteristics of rectangular cross-section microchannels were better than those of triangular and trapezoidal cross-section microchannels (Figs. 1a, b), but there was no detailed comparative analysis of the reasons for this difference. Vinoth and Senthil Kumar [12] investigated the heat transfer and hydrodynamic properties of inclined fin MCHS with different channel cross-sections (Fig. 1c). The trapezoidal cross-section microchannel has better performance than the square and semi-circular cross-sections, where the heat transfer rate increases by 8.5% and 10.3% compared to the square and semi-circular cross-sections, but the pressure drop is the highest of the three cross-section microchannels. Unlike previous studies, the authors have analyzed the reasons why trapezoidal section flow channels have the highest heat transfer capacity and the main reason for this is that trapezoidal section micro flow channels have the highest heat transfer area. In addition, the authors show that the greatest pressure drop in trapezoidal microchannels is caused by the increased coefficient of friction due to the characteristics of their structure.

The following studies compare more microchannels with different cross-sectional shapes than those described above. Moradikazerouni et al. [13] investigated the thermal performance of five air-cooled MCHS with different inlet cross-sections for supercomputer cooling applications (Fig. 2). Considering the inlet hydraulic diameter, the heat transfer performance of triangular and straight slot shaped microchannels is better than that of hexagonal and other shaped microchannels, but they also have the greatest pressure drop due to the increased coefficient of friction. Moreover, considering the difficulty of manufacturing triangular microchannels, a straight slot shaped channel was chosen to achieve heat dissipation. To provide a more comprehensive analysis of the reasons for the differences in

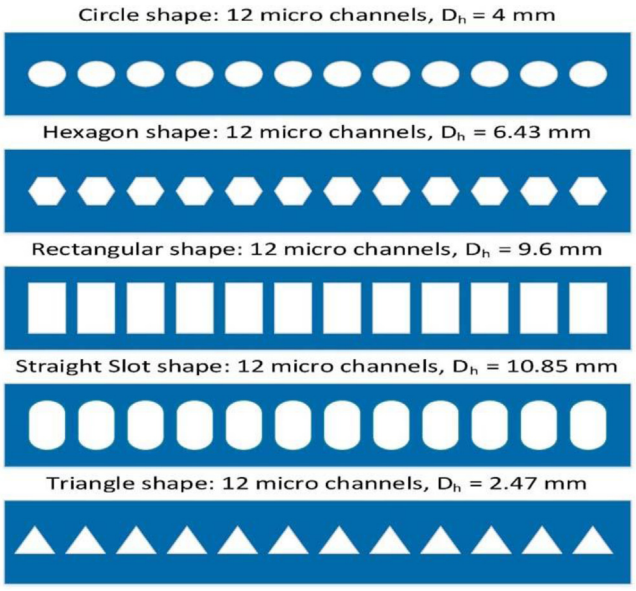

Fig. 2. Five different inlet cross-section shapes for microchannels [13].

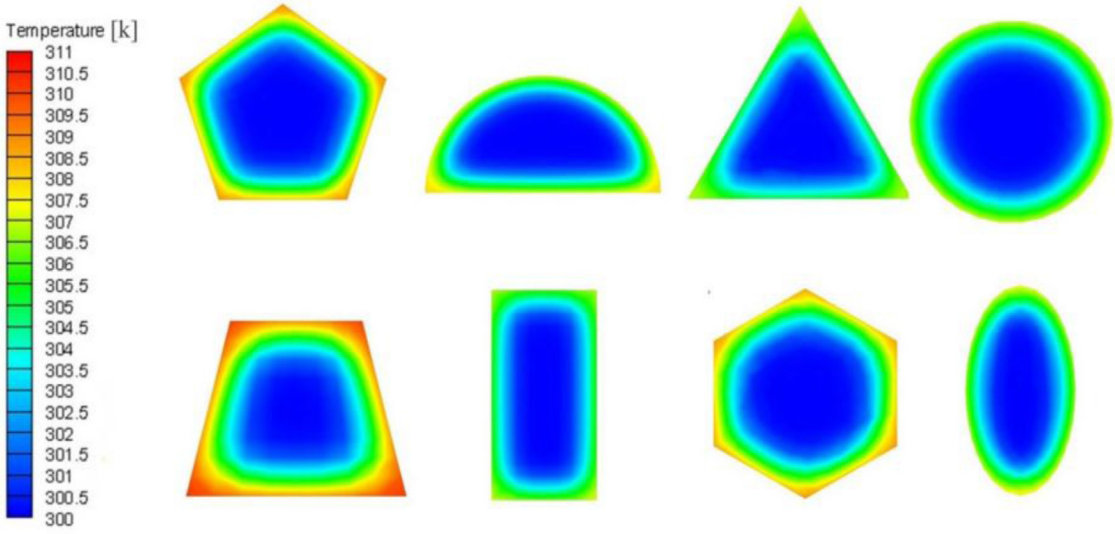

Fig. 3. Eight different cross-sectional microchannel temperature distribution clouds [14].

heat transfer performance caused by different cross-sectional shapes. Alihosseini et al. [14] numerically simulated 15 microchannels with different cross-sectional shapes and presented the temperature distribution clouds for eight different cross-sectional shapes with better temperature distribution (Fig. 3), where the circular cross-sectional shape has few hot spot areas and uniform temperature distribution. It can also be seen that the trapezoidal cross-section shape has the lowest heat transfer efficiency, mainly because of the dead zone and zero velocity point at the acute angle of the trapezoidal cross-section, which affects the heat transfer efficiency. Furthermore, the increase in fluid inlet velocity is a possible reason for the lower heat transfer performance of the trapezoidal cross-section. Based on the results of these studies, it can be found that microchannels with different cross-sectional shapes have greater differences in heat transfer performance, among which triangular and trapezoidal cross-sectional microchannels currently exhibit the best heat transfer characteristics, but this also depends on the specific inlet flow rate range and the size of the cross-sectional area of the channel. At the same time, the better heat transfer performance generally depends on the actual heat transfer area of the runner, but it is also affected by the flow dead zone in the channel.

2.2 Bionic structured microchannels

The advantage of bionic MCHS is that they can enhance fluid flow by taking inspiration from various animal and plant structures found in nature, such as leaf veins, plant

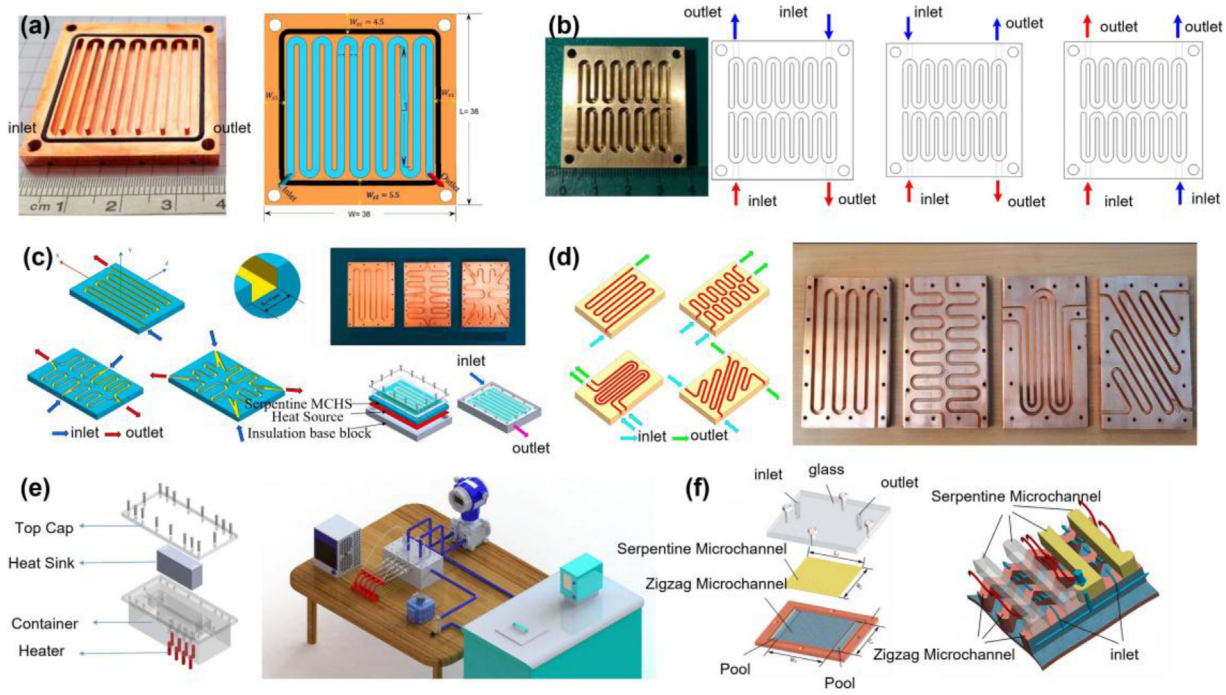

Fig. 4. Various types of serpentine channel distribution (a) Traditional serpentine channels [16] (b) Symmetrically distributed serpentine channels [17] (c) Conventional, orthogonal and diagonal arrangement serpentine channels [18] (d) Four different distributions of serpentine channels [19] (e) Serpentine channels for CPU applications [20] (f) Combination of serpentine channel and zigzag channels [21].

roots and shark skin, to improve temperature uniformity and heat transfer performance. In terms of conjugate heat transfer, bionic optimization is often used for the design of microchannel structures, but this optimization method is not yet mature enough. This section provides a review and analysis of recent research on bionic structures in microchannel design. The serpentine flow channel has been used by most researchers for its simple structure and good heat transfer characteristics. In earlier years, Hao [15] and Al-Neama [16] successively analyzed the heat transfer and flow characteristics of serpentine MCHS (Fig. 4a). The heat transfer performance of the serpentine microchannel is superior to that of the linear microchannel, where the former can reduce the temperature of GaN HEMT devices from 124.7 °C to 96.7 °C, mainly because the fluid flow at the serpentine bend can break the thermal boundary layer to enhance the heat transfer performance. To increase the heat dissipation area and enhance the bending disturbance in the serpentine channel, many researchers have improved the design of the serpentine channel structure. For example, Cao [17], Jaffal [18] and Imran [19] carried out numerical and experimental analyses of the heat transfer and hydraulic characteristics of serpentine flow channels with different inlet and outlet locations and distribution methods (Figs. 4b–d). The new design of the serpentine channel changes the previous structure of single inlet and single outlet to a two-inlet and two-outlet distribution, which results in a more fragmented flow channel with more curved features. In the experimental analysis, the newly designed serpentine channel can significantly increase the Nusselt number by 32.6%, and the smaller the heat sink volume, the higher the heat transfer coefficient, which can be increased by a maximum of 1.23 times. This indicates that the fluid disturbance caused by the curved features of the serpentine channel is the key to improving the heat transfer performance of the heat sink. In practical cooling applications, Gorzin et al. [20] compared the heat transfer performance of serpentine and conventional straight microchannels for CPU cooling requirements. The temperature of the serpentine microfluidic base plate was reduced by 11.2% compared to the linear microfluidic base plate, which significantly reduced the CPU operating temperature (Fig. 4e). Peng et al. [21] proposed a dual-layer MCHS structure combining serpentine microchannels and zigzag microchannels (Fig. 4f), and its heat transfer performance and temperature uniformity were substantially improved compared to the conventional serpentine microchannels.

The tree-like structure includes multiple microchannel branches. The main fluid is dispersed into each branch fluid, and each branch fluid is then dispersed into the next level of branches, filling the entire MCHS step by step. These characteristics of branching and merging provide a reference value for the design of MCHS. Chen and Cheng [22] and Zhang [23] investigated the flow properties and heat transfer performance of double-layer tree-shaped MCHS (Fig. 5a). The pumping power required for the tree-shaped microchannels under all studies is significantly smaller than that of the parallel and serpentine microchannels, which effectively reduces energy losses. In the heat transfer performance analysis, the dendritic MCHS has a lower maximum temperature and better temperature uniformity, resulting in a significant improvement in temperature control.

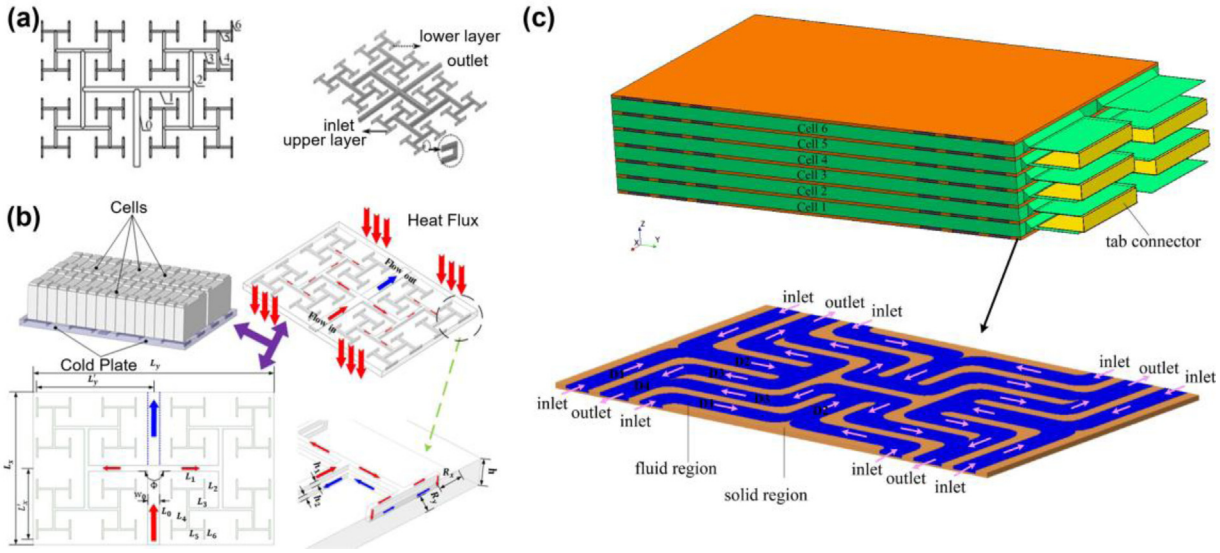

Fig. 5. Tree-shaped microchannel structure (a) Double layer tree-shaped microchannels [23] (b) Tree-shaped microchannels for battery heat dissipation [24] (c) New tree-shaped microchannel structure [27].

Fan et al. [24,25] applied dendritic microchannels to the heat dissipation of an electric vehicle battery (Fig. 5b). Compared to serpentine microchannels, the optimized tree-shaped microchannels could reduce the surface temperature difference by 69.25%, while generating a pressure drop that was 20.87% of the pressure drop in a serpentine channel under the same conditions. Shui et al. [26] carried out a study on the flow and heat transfer performance of a bionic tree microchannel with a T-shaped branching structure. The tree structure was graded along the axial direction, which is simpler than the microchannel structure studied above. In numerical simulations, the tree-shaped microchannel effectively promotes fluid mixing. In particular, the secondary flows formed at the T-shaped bifurcation structure, including impinging jets and vortices, can significantly enhance heat transfer. Ran et al. [27] similarly constructed a novel dendritic MCHS for the thermal management of automotive batteries (Fig. 5c). This heat dissipation plate can control the temperature difference of the battery within a range of 1 °C, which is smaller than the minimum temperature difference of 1.96 °C for the cold plate studied by Fan et al. [25]. One possible reason for this difference is that the new tree-shaped microchannel has a rounded transition at the bifurcation, which effectively prevents uneven temperature distribution due to localized flow dead zones in the bifurcation. Based on the above studies, it is shown that the branching and merging flow method of the tree structure distributes the fluid medium throughout the heat source, which is the reason for increasing the overall temperature uniformity and improving the heat transfer efficiency of the microchannel. However, due to the complexity of the tree-shaped structure, it is difficult and costly to manufacture. Current research is still based on numerical simulations.

The bionic leaf vein network microchannel has also been the focus of researchers studying microfluidic heat sinks in recent years due to its excellent flow properties and heat transfer performance. The structure is similar to the tree-shaped microchannel and has the same characteristics of branching and merging. Luo et al. [28] designed and fabricated a bionic leaf vein network microchannel vapor chamber for heat dissipation of optoelectronic products, referring to the macroscopic leaf vein network structure and the microscopic leaf flesh tissue structure (Fig. 6a). Due to the greater permeability and capillary suction of this vein structure, the temperature uniformity of the cavity surface is significantly improved. Li et al. [29] used a topology optimization method to design two types of leaf-veins MCHS with the objectives of lowest fluid power consumption and optimal heat transfer performance, respectively, and compared the flow performance and heat transfer performance with the conventional serpentine microchannel (Fig. 6b). The surface temperature of the microchannel designed with the goal of maximum heat exchange is the lowest, and the pressure drop of the microchannel designed with the goal of fluid power consumption is the smallest because its flow distribution is more reasonable. Tan et al. [30] proposed second and third order vein-shaped microchannel structures based on the idea of leaf vein bionics, which provide better heat transfer and temperature uniformity compared to linear microchannel structures. Under the condition that the cross-sectional area of the microchannel remains unchanged, the number of microchannels at the local hot spot is improved, and asymmetric second order and third order vein microchannels are obtained (Fig. 6c). In general, the temperature uniformity of the third order microchannel is better than that of the second order, and the minimum temperature deviation is 1.8 °C. Peng et al. [31] also investigated symmetrical and asymmetrical bionic leaf vein microchannels with different leaf vein branching angles (Fig. 6d). Compared with the two-stage vein network microchannels, the three-stage vein network microchannels have larger heat transfer areas and more uniform flow distribution. At the same time, the smaller branch angle of the asymmetric vein has a better heat

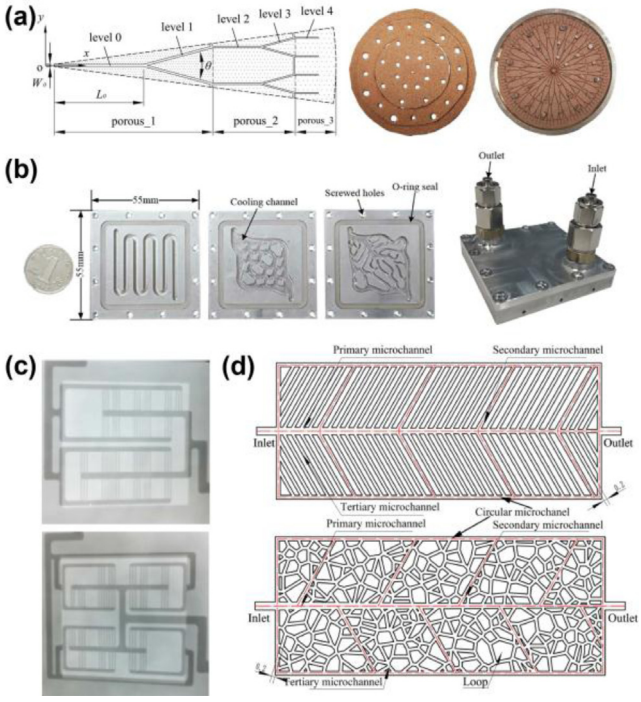

Fig. 6. Leaf vein network microchannels (a) Fractal leaf vein network structure [28] (b) Leaf-vein MCHS after topology-optimized design [29] (c) Asymmetrical second and third order leaf vein microchannels [30] (d) Symmetrical and asymmetrical three-stage leaf vein microchannels [31].

transfer performance. All the above studies show that the vein structure has a very significant effect on enhancing the heat transfer performance of the heat sink. In addition, the heat transfer characteristics are mainly influenced by the branching grade and branching angle of the leaf veins, where the heat transfer performance of third order leaf vein microchannels is generally better than that of second order ones. The branching level currently studied mainly stays at the third order, and it is worth investigating whether the vein structure of the fourth or even higher branching level is more advantageous for enhancing heat transfer performance.

Spider web is a network topology with excellent characteristics in nature, and it has a significant effect in increasing the heat exchange area. Tan et al. [32] designed MCHS with four different topologies including trigonal veins, side veins, snowflake and spider web structures to address the problem of thermal failure in high heat flow density chips, of which the spider web microchannel (Fig. 7a) has the best performance, mainly because of the uniform mixing of fluids in the spider web microchannel, which covers the entire channel and increases the actual heat transfer area of the channel. Based on the study carried out by Tan et al. [32] on bionic topology in the thermal management of single-phase flows, Tan et al. [33] proposed and optimized a spider-web MCHS in heat transfer experiments to improve local temperature unevenness. Figure 7b shows the spider-web microchannels before and after optimization. The optimized spider-web microchannel has a temperature standard deviation of 1.58 °C when the heat flux density is 100 W/cm^2. Compared with the 2.23 °C of the third order bionic leaf vein microchannel under the same heat flux density, the temperature uniformity is greatly improved. Considering the better effect of the two-in-two-out flow method in enhancing heat transfer in previous serpentine flow channel studies, Han et al. [34] proposed a three-in-three-out spider-web microchannel structure (Fig. 7c), which is effective in regulating flow uniformity and enhancing fluid mixing. The heat sink of this structure significantly improves temperature uniformity and reduces convective thermal resistance, with a 57.35% reduction in temperature difference compared to conventional spider-web shaped MCHS. The spider-web shaped microchannels cover a large area and have the flow bending characteristics to dissipate heat at high heat flux densities. However, the spider web structure is complex and difficult to manufacture, and current research tends to use topology optimization methods to improve the spider web structure.

The application of bionics in MCHS is not limited to those mentioned above, and many researchers have investigated different bionic structures. For example, Hu et al. [35] applied a topology optimization method to design a biomimetic bifurcated river MCHS. Compared with the traditional linear microchannel structure, the topological bionic bifurcation structure has the characteristics of bifurcation and merging, and the optimized microchannel can reduce the pressure drop by 0.6KPa and the heat source temperature by 4 °C. Wang et al. [36] designed a bionic rough-walled rectangular microchannel with a hydraulic diameter of 1000 μm based on a dragonfly wing structure, as shown in Figure 8a. The heat transfer performance of the bionic wall microfluidic structure is superior to that of a smooth rectangular microfluidic channel. The main reason for this is that the bionic wall structure increases the flow velocity and enhances the disturbance of the fluid in the flow channel, which promotes

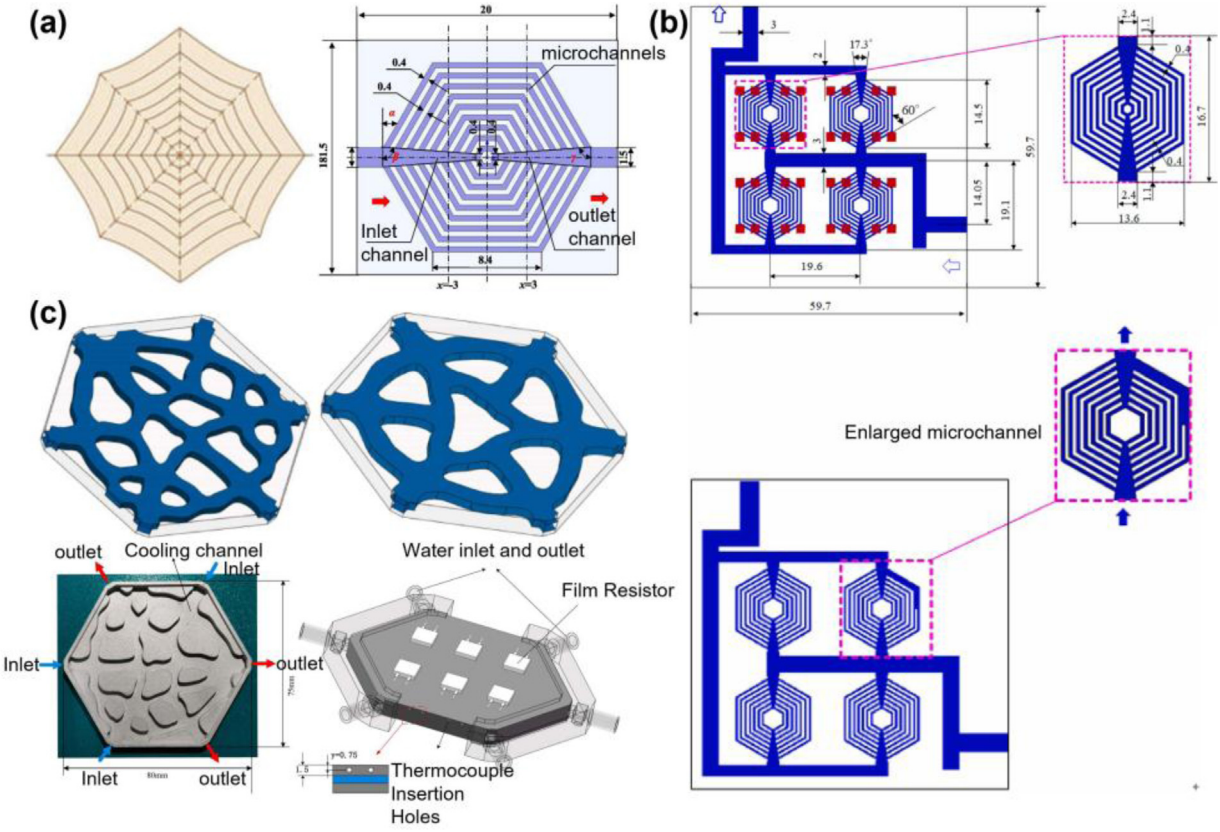

Fig. 7. Spider-web microchannels (a) Spider-web microchannels for high heat flux density chip thermal management [32] (b) Spider-web microchannels for phased-array antenna thermal management before and after optimization [33] (c) Three-in-three-out spider-web microchannel structure [34].

the generation of many vortices in the flow channel, thus enhancing the convective heat transfer performance. Inspired by the sharkskin bionic concept, Li et al. [37] proposed four novel bionic MCHS for improving the flow and heat transfer characteristics of water-cooled microchannels (Fig. 8b). The bionic sharkskin structure diffuses the cooling fluid into the sidewalls, which can reduce the thickness of the thermal boundary layer at the sidewalls and improve the overall temperature uniformity of the microchannel. Also, the continuous contraction and expansion of the fluid facilitate the heat exchange between the fluid and the wall, significantly enhancing the heat transfer performance. Wang et al. [38] conducted an experimental study on the heat dissipation of a wave shaped MCHS. The greater the wave amplitude and the shorter the wavelength, the greater the microchannel heat transfer area, but an increase in the number of waves also results in greater flow resistance. Therefore, it is necessary to ensure a lower flow resistance to reduce pumping power losses while considering the thermal performance.

2.3 Reinforced rib structure

Conventional smooth flow channel structures have poor heat transfer performance and uneven temperature distribution due to the thick thermal boundary layer. In recent years, reducing the total thermal resistance by improving the design of the microchannel structure to enhance heat transfer has been the focus of research. The design of the reinforcing rib structure in the channel can not only increase the heat transfer surface area of the microchannel but also can re-develop the thermal boundary layer by interrupting the fluid flow. In particular, the heat transfer performance is enhanced by promoting the mixing of hot and cold fluids. Meanwhile, the reinforced rib structure increases the pressure drop in the microchannels, which requires higher pumping power.

2.3.1 Sidewall rib structure

Adding rib structures to microchannels not only increase the heat transfer area but also enhance the fluid disturbance, which plays a very effective role in enhancing heat transfer. In addition, different rib shapes have different degrees of improvement in heat transfer performance. As early as ten years ago, Zhang et al. [39] found that the heat transfer capacity of microchannels with different rib shapes was higher than that of traditional smooth microchannels (Fig. 9a). Meanwhile, the heat transfer performance of the microchannels with triangular and semicircular fins is similar and higher than that of the microchannels with rectangular fins. Behnampour et al. [40] studied the effect of triangular, rectangular and trapezoidal ribs on the hydraulic and heat transfer

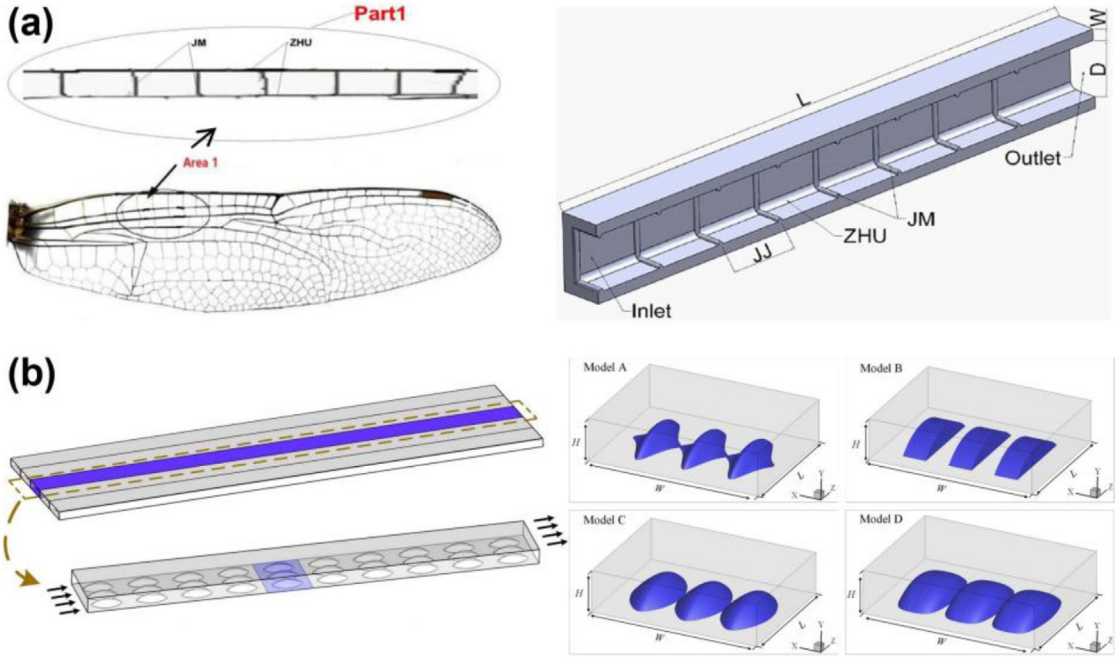

Fig. 8. Different bionic MCHS (a) Bionic dragonfly wings rectangular MCHS [36] (b) Bionic shark skin MCHS [37].

characteristics (Fig. 9b). The fluid flowing through the trailing edge of each rib can generate different sized vortices, which can effectively weaken the thermal boundary layer. The trapezoidal rib microchannel has the highest Nusselt number, while the triangular rib microchannel has the lowest inlet and outlet pressure drop. To address the issue of balancing heat transfer capacity and hydraulic performance in engineering, the author has defined a thermal performance evaluation criterion (PEC) to assess the best performance of MCHS with different ribs, among which the triangular rib micro-runner has the highest PEC value. The PEC is defined as:

$$PEC = \frac{\frac{Nu_{ave}}{Nu_{0ave}}}{\left(\frac{f}{f_0}\right)^{1/3}} \quad (1)$$

where Nu is the Nussle number; f is the coefficient of friction of the channel; N_{u0} is the Nussle number of smooth rectangular microchannel; f_0 is the coefficient of friction of smooth rectangular microchannel.

Both above studies show that the triangular rib structure has better comprehensive performance for improving heat transfer. Therefore, in the design of microchannels with interrupted disturbance structures, triangles can be considered as the inner rib structure of the channel.

In subsequent studies, researchers have investigated more different shapes of ribs in terms of enhanced heat transfer properties. Rehman et al. [41,42] carried out a numerical study of the heat transfer and hydraulic characteristics of elliptical, trapezoidal, hydrofoil-shaped and rectangular ribbed microchannels. The addition of sidewall ribs improves the heat transfer performance, among which the hydrofoil-shaped rib microchannel has the best heat transfer performance and its pressure drop is the lowest among all sidewall rib microchannels. The average heat transfer coefficient can be effectively increased by 26.3%. Then the author studies the different geometric parameters of the hydrofoil-shaped ribs, such as the height, width and spacing between the hydrofoils (Fig. 9c). Numerical analysis shows that the heat transfer performance becomes higher as the hydrofoil rib width increases, the height increases and the spacing becomes smaller. However, a greater number of hydrofoil ribs leads to a continuous contraction and expansion of the fluid, creating an obstruction to the fluid flow and resulting in an increase in pressure drop. Chai et al. [43–45] analyzed the heat transfer performance of fan-shaped sidewall rib microchannels (Fig. 9d). The greater the height of the fan-shaped ribs and the smaller the spacing between the fan-shaped ribs, the microchannel performs better heat transfer. The numerical analysis also found that the heat transfer performance of the aligned fan-shaped rib microchannels was better than that of the offset fan-shaped rib microchannels. The Nusselt number increases of these two types of microchannels range from 6% to 101% and 4% to 103%, respectively, mainly because the aligned rib microchannels can effectively interrupt the fluid flow, while the offset rib microchannels only can interrupt part of the fluid. In recent years, there has also been a discussion on whether the rib with rounded corners can improve heat transfer performance and hydraulic performance. For example, Derakhshanpour et al. [46] conducted a heat transfer and hydraulic performance analysis of semicircular and semi-elliptical rib-shaped microchannels and analyzed the effect of fillet on heat transfer performance (Fig. 9e). Numerical analysis shows that the semi-elliptical rib filleted microchannel has the best heat transfer performance, but the

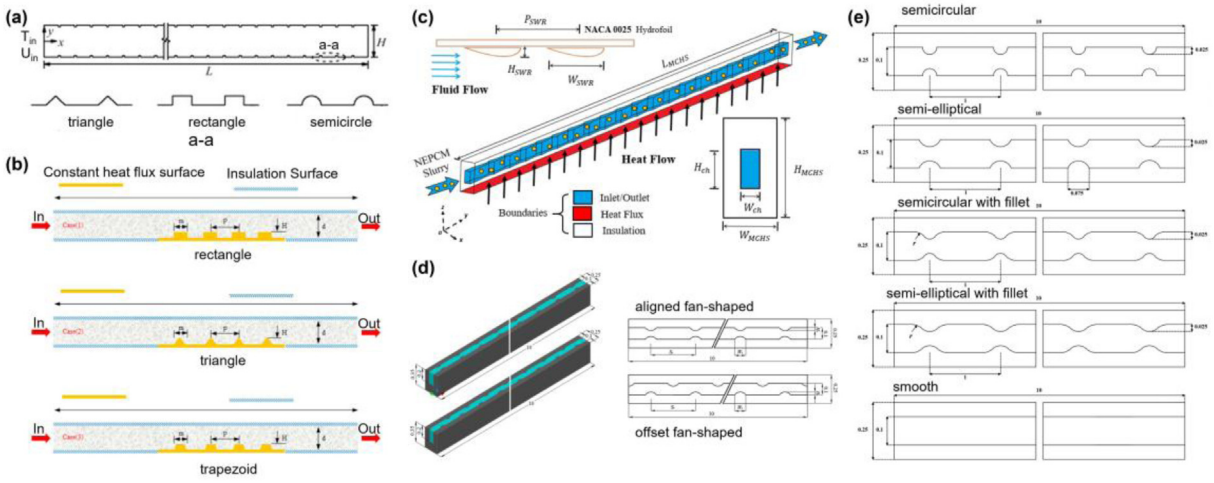

Fig. 9. sidewall rib structure (a) triangular, rectangular and semi-circular sidewall ribs [39] (b) Triangular, rectangular and trapezoidal sidewall ribs [40] (c) Hydrofoil-shaped sidewall ribs [42] (d) Aligned and offset fan-shaped sidewall ribs [43] (e) Semicircular and semi-elliptical sidewall ribs with or without fillet [46].

semicircular rib filleted microchannel has the highest PEC. The addition of fillets can effectively reduce the low velocity zone of the downstream fluid and promote the mixing of the hot flow near the wall and the cold fluid in the center of the channel. Based on the above studies, it is found that the commonality of different rib shapes is that they can interrupt the fluid flow and redevelop the boundary layer, but the size and number of flow dead zones existing in different ribs are different. Summarizing the above research results, the heat transfer performance of the ribs with the curved structure is more prominent than others. In addition, the rib structures in the channel are very difficult to machine, leading to a sharp increase in manufacturing costs. As a result, current research is also dominated by simulation.

2.3.2 Fin structure

The addition of rectangular finned ribs in MCHS will also play a considerable role in improving heat transfer performance. Adhikari et al. [47] conducted a numerical study of the effect of the length parameter of rectangular straight fins on the heat transfer performance in convection experiments. The short rectangular straight fins can effectively reduce the thickness of the thermal boundary layer, and the heat transfer efficiency is significantly higher than that of long rectangular straight fins. This is similar to the results obtained by Ben Hamida and Hatami [48] in their experiments on heat dissipation of light-emitting diodes. Ali et al. [49] innovatively conducted thermal analysis on the inclination and spacing of rectangular fins. The addition of rectangular fins can effectively enhance the heat transfer rate of the microchannels, where the best heat transfer performance is achieved at a fin inclination of 75° and a larger fin spacing. The main reason for the increase in heat transfer performance is that the vortex formed at the rib can promote the secondary flow, which distorts the growth of the thermal boundary layer and weakens the thermal boundary layer.

The arrangement of the above-mentioned ribs is concentrated on a horizontal line and is relatively regular. In more studies, Sun et al. [50] innovatively proposed a cross-arranged ribbed microchannel. The microchannels have three main shapes of rib structure including MCHSs imitating Tesla valve (MCTV), mounted with sector bump (MCSB) and diamond bump (MCDB), which were compared with parallel straight microchannels at the same heat transfer area in terms of heat transfer performance and flow properties. The heat transfer performance of the three MCHSs with ribbed structure is better than that of MCSC because these MCHSs can induce flow separation and the existence of secondary flow channels promotes fluid mixing to form vortices, resulting in periodic interruption and development of thermal boundary layers. Among the three ribbed MCHS, the MCSB has the best heat transfer performance of the three structures due to the significantly greater number of vortices generated by fluid mixing (Fig. 10), which allows the temperature of electronic components to be controlled within 70 °C. Different from previous studies, Zhang et al. [51] first proposed microchannels containing aligned and staggered rib structures to enhance heat transfer, as shown in Figure 11. The introduction of ribs can significantly improve cooling performance by disrupting and redeveloping the thermal boundary layer. The staggered rib design also provides better heat transfer performance than the aligned rib design, with an average temperature reduction of 6.75% and an improvement in temperature uniformity of 0.005 compared to a straight MCHS.

Circular pin fins have also been shown to be remarkably effective in changing the fluid state, increasing fluid disturbance and improving heat transfer performance. Wang et al. [52] investigated the heat transfer performance of microchannels containing only one single pin fin under single-phase flow. The presence of the pin fin splits the fluid medium into two accelerated flows, and then the mixing of the fluids promotes vortex shedding at the trailing edge of

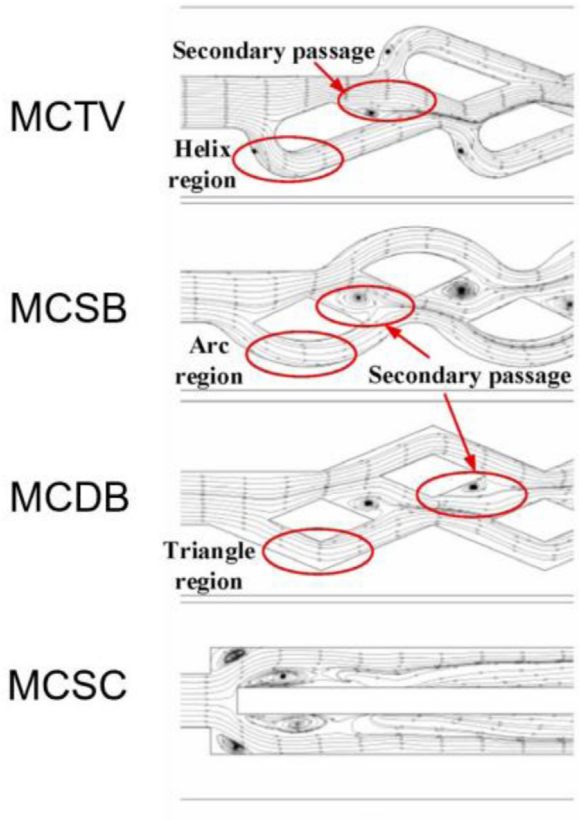

Fig. 10. Streamline distribution of cross-arranged ribbed microchannels [50].

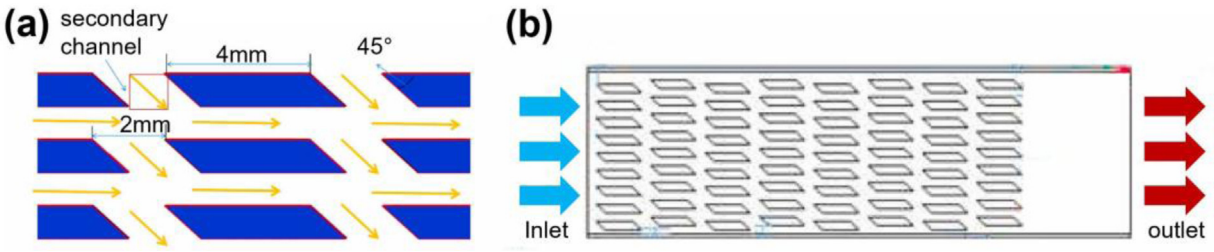

Fig. 11. Microchannel heat sink with ribs [51] (a) Aligned rib microchannels (b) Staggered rib microchannels.

the pin fin (Fig. 12a). To investigate the effect of multiple cylindrical pin fins on the overall heat transfer performance and hydraulic performance of the microfluidic heat sink, Vasilev et al. [53] analyzed the heat transfer performance of the MCHS with multiple parallel arranged cylindrical pin fins (Fig. 12b). The addition of the pin fins increases the heat transfer area. At the same time, the vortex formed by the fluid medium at the trailing edge of the pin fins increases the disturbance and promotes heat dissipation. The maximum Nussle number increment of the heat sink in this microchannel is four times that of a smooth microchannel. However, the reduction in flow cross-section also increases pressure drop, so the overall performance is often assessed using PEC. Lyu et al. [54] designed a novel circular bionic pin-fin heat sink based on the phylogenetic theory of biology. The bionic configuration of the pin-fin has better uniformity and complementarity, and the airflow channel is more reasonable, which can reduce the surface temperature of the thermal block by 14.7%. Yan et al. [55] found that narrow microchannels embedded with cylindrical pin fins can significantly enhance the heat transfer capability of the chip, and its ability to improve temperature uniformity was measured by multiple hot spots. The diameter of the circular pin fins is distributed in a gradient along the runner, which significantly enhances the local heat dissipation of the chip and improves the temperature uniformity on the chip surface (Fig. 12c). The diameter of the circular pin fins is distributed in a gradient along the channel, which significantly enhances the local heat dissipation of the chip and improves the temperature uniformity on the chip surface. Pan et al. [56] proposed a cylindrical pin-fin manifold MCHS (Fig. 12d). The fluid flows from top to bottom and is separated by multiple partitions, which is rare in previous studies. Under the

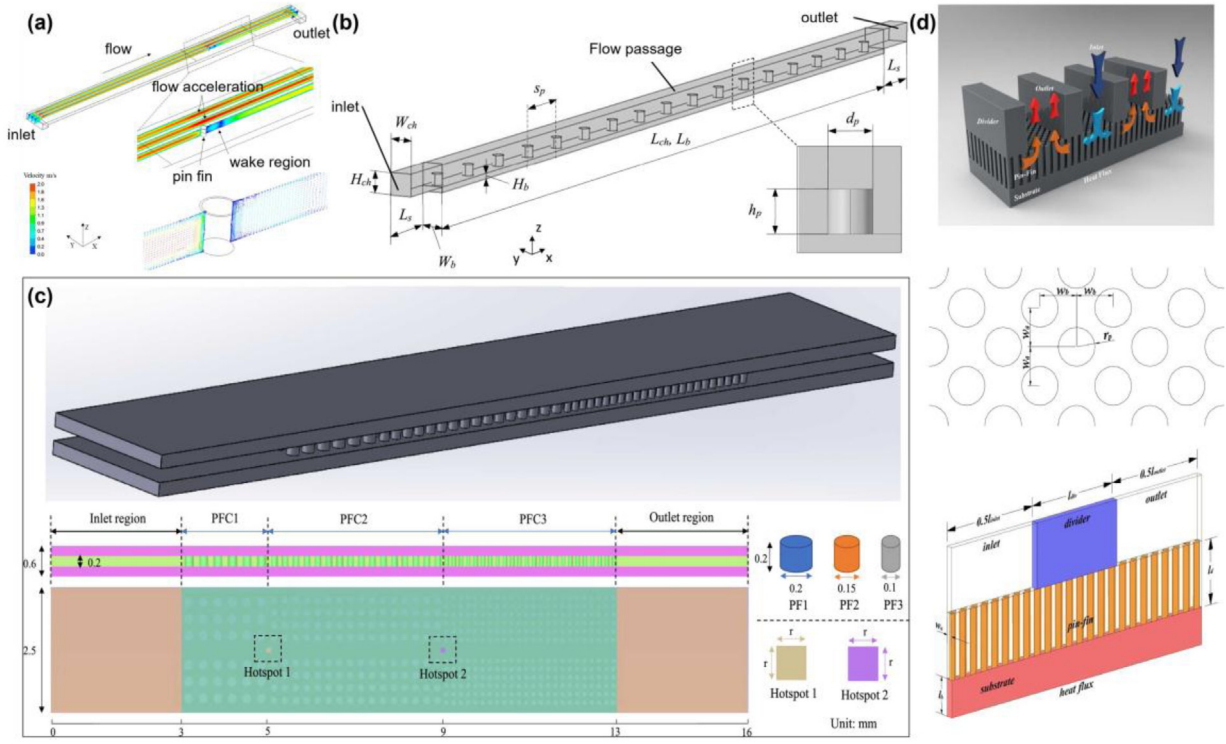

Fig. 12. Cylindrical pin fin construction (a) x-z plane velocity vector cloud of the microchannel with single cylindrical pin fin [52] (b) Plurality of horizontally parallel arranged cylindrical pin fin structures [53] (c) Variable diameter cylindrical pin fins [55] (d) Cylindrical pin-fin manifold MCHS [56].

same mass flow rate, the cylindrical pin-fin MCHS structure has a better heat transfer performance than the rectangular MCHS structure, mainly because the disturbance effect caused by the pin fins contributes to the enhanced heat transfer. All above studies on cylindrical pin fins have demonstrated that cylindrical pin fin structures can significantly enhance heat dissipation. However, due to the difficulties of manufacturing, the basic research is based on simulation.

The addition of cylindrical pinned fin structures can effectively improve the heat transfer performance of microfluidic heat sinks, but Sreehari and Prajapati [57] et al. have proposed a rhombic shaped column fin structure to compare the heat transfer performance and hydraulic performance with the cylindrical fin structure. The maximum Nusselt number of rhombic fins is 40% higher than that of circular fins. The net effective heat transfer area of the rhombic structure is higher than that of the cylindrical structure, and the larger heat transfer area promotes stronger heat dissipation. Further, the vortex created by the trailing edge section of the rhombic structure promotes better coolant exchange in the flow channel and weakens the development of the thermal boundary layer. However, the presence of sharp edges in the rhombic structure forces the fluid to become disturbed, which produces a higher pressure drop than in the cylindrical structure. Jia et al. [58] investigated the heat transfer and fluid flow characteristics of tapered fin microchannels with different fin arrangements (Fig. 13). Numerical analysis showed that the arrangement with tapered fins distributed throughout the microchannel has the best heat transfer performance and the best temperature uniformity, which is due to the larger heat dissipation area of the microchannel in this arrangement and the more intense flow separation and mixing.

2.3.3 Rib structure varying in height direction

The rib structures described above mainly focus on the changes in the two-dimensional plane, but fewer studies have been carried out on the improvement of heat transfer performance and hydraulic properties by varying the rib shape in the height direction. Zheng et al. [59] proposed a hierarchical MCHS, which mainly includes three different hierarchical pin fins (Fig. 14), labeled as U-type, M-type and D-type pin fins, and compared with traditional T-type pin fins. The U-shaped pin-fin structure MCHS shows the best heat transfer performance among the four structures due to its largest top size, which increases the flow rate at the heat source and reduces the conduction heat resistance. Wang et al. [60] designed a bidirectional ribbed (BR) MCHS by combining vertical ribs (VR) and spreading ribs (SR) (Fig. 15), and the heat transfer and hydraulic analysis of the MCHS were carried out for all three rib structures. BR microchannels can promote the generation of more circulating flow, which can create a wider range of hot and cold fluid impingement and mixing, effectively interrupting the development of the thermal boundary layer. Further, the addition of BR forms a larger heat dissipation area. It can be seen from the above two

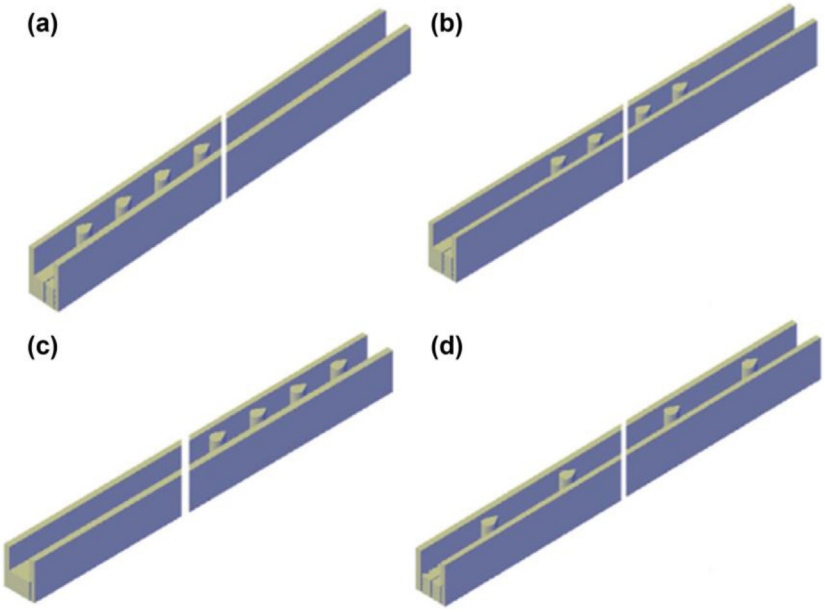

Fig. 13. Tapered fin structure in different arrangements [58] (a) Upstream layout (b) Intermediate layout (c) Downstream layout (d) Distributed throughout the microchannel.

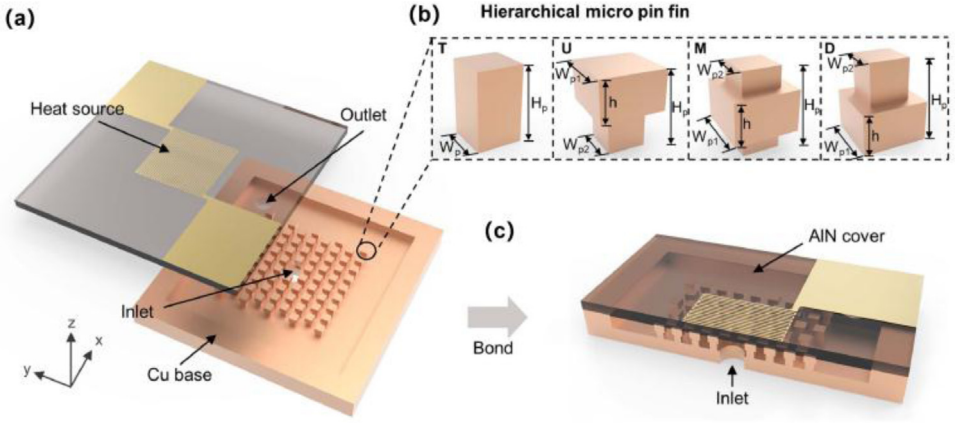

Fig. 14. Schematic diagram of microchannel heat sinking [59] (a) Overall structure of heat sink with staggered micro pin fins (b) Three different hierarchical micro pin fins (c) Cross-sectional view of MCHS.

studies that the larger size of the top ribs can not only increase the flow velocity of the fluid at the heat source but also lead to more severe disturbance. This design can significantly enhance the heat transfer, which is different from the traditional rib structure with the same structure in the height direction.

2.4 Concave cavity structure

In recent years, the research on the concave cavity in the microchannel mainly focuses on the effect of different cavity structures on the heat transfer performance and the application of the combination of the concave cavity and bionics in the microchannel. The function of the cavity structure is similar to that of the rib structure, which increases the heat transfer area while promoting fluid disturbance and enhancing heat transfer.

2.4.1 Different concave cavity structures on the walls

The original design purpose of the cavity structure is to increase the heat dissipation area of the MCHS, but most of the traditional cavity structures used to increase the heat transfer area usually exist in the design of rectangular parallel microchannels. The concave cavity structures currently studied are also used in bionics. For example, Chen et al. [61] proposed a serpentine concave cavity microchannel (Fig. 16). The serpentine concave microchannel not only has a larger heat dissipation area but also can effectively disturb the development of the thermal boundary layer and promote the mixing of fluids.

Further, the research on the cavity structure MCHS mainly focused on the effect of the cavity to interrupt the fluid and enhance the heat transfer. For example, Chai et al. [62] conducted heat transfer studies on MCHS with an offset

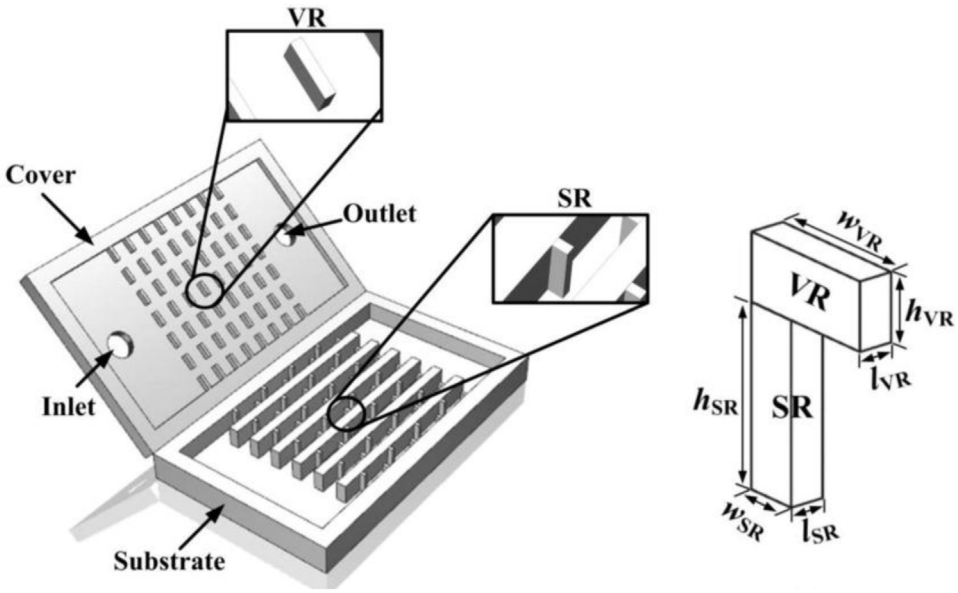

Fig. 15. MCHS with BR [60].

fan-shaped concave cavity structure (Fig. 17a) and showed that the offset fan structure improved the heat transfer performance within an acceptable pressure drop. In the same year, Xia et al. [63] investigated the heat transfer performance of triangular concave cavity MCHS with the same flow channel dimensions (Fig. 17b). The results show that the vortices within the triangular concave cavity greatly enhance the mixing of convective fluids, which interrupts the thermal and hydraulic boundary layer developing along the channel and enhances the heat transfer in the constant cross-section. However, the two studies mentioned above were not compared with each other to analyze the advantages and disadvantages. Li et al. [64] also investigated the heat transfer characteristics of triangular concave cavities and reached similar conclusions (Fig. 17c), but different from the previous studies, the fluid medium in this study used nanofluids. Kumar [65] compared the Nusselt number and Poiseuille number of arc-shaped grooved microchannels under four different distributions (Fig. 17d). The addition of the arc groove can increase the Nusselt number by up to 119%, but it also leads to an increase in the Poiseuille number, which indicates a significant increase in pressure drop. In addition, studies have shown that the smaller the depth of the arc groove, the better the heat transfer efficiency, especially at low Re. Xia et al. [66] designed MCHS with a smooth rectangular structure, offset fan-shaped cavity structure and offset triangular cavity structure, respectively (Fig. 17e). The offset fan and offset triangular concave cavity structures have a large heat transfer area compared to the rectangular structures. In addition, the jet and throttle effects caused by regular flow expansion and contraction at the inner wall of the flow channel can promote secondary flow and mixing disturbances, contributing to the interruption and redevelopment of the flow boundary layer. Under the heat flux input of 200 W/cm^2, the maximum temperature can be controlled below 326 K. All the above studies have shown that the triangular concave cavity has significant advantages for improving heat transfer. Subsequently, Zhu et al. [67] carried out a more detailed comparative analysis of flow heat transfer for MCHS with triangular grooves and other shaped sidewall grooves in the Re range of 190–610 (Fig. 17f). The addition of grooves can cause the generation of vortices, which can promote the mixing of hot and cold fluids and enhance heat exchange. Among them, the triangular grooved microchannel has the highest Nusselt number. In addition, the concave cavity promotes the transition of the fluid to the rolling flow mode, which can effectively reduce the pressure drop. The triangular grooved microchannel has the highest synergy degree of velocity field and temperature field, indicating its highest comprehensive performance. Similar results are found in the numerical simulation of conventional rectangular, trapezoidal, fan-shaped, and rectangular concave cavity MCHS by Pan et al. [68].

Based on the results of Pan et al. [68], Pan et al. [69] further analyzed the heat transfer performance of MCHS with different deviations and distribution methods for fan-shaped concave cavities (FSCs) in the Re range of 12.20–123.31. There exists an optimum deviation of FSCs to optimize heat transfer performance, which is largely dependent on the effect of fluid disruption and disturbance. Meanwhile, FSCs have the best heat transfer performance in the case of dense distribution in the front and sparse distribution in the back (Fig. 17g). Bi et al. [70] performed numerical simulations of convection cooling heat transfer in the larger Re range of 2700–6100 for MCHS with dimples, cylindrical grooves and low fins (Fig. 17h). To comprehensively compare the heat transfer performance and pressure drop loss between the MCHS, the study defined the PEC for evaluation. The results show that the magnitude of Re has a significant effect on the PEC value of the microchannels with dimples. When $Re < 3323$, the PEC value of the cylindrical grooved MCHS is the largest, but when Re increases, the PEC value of the grooved MCHS exceeds that of the cylindrical grooved MCHS. Based on the above studies, it is

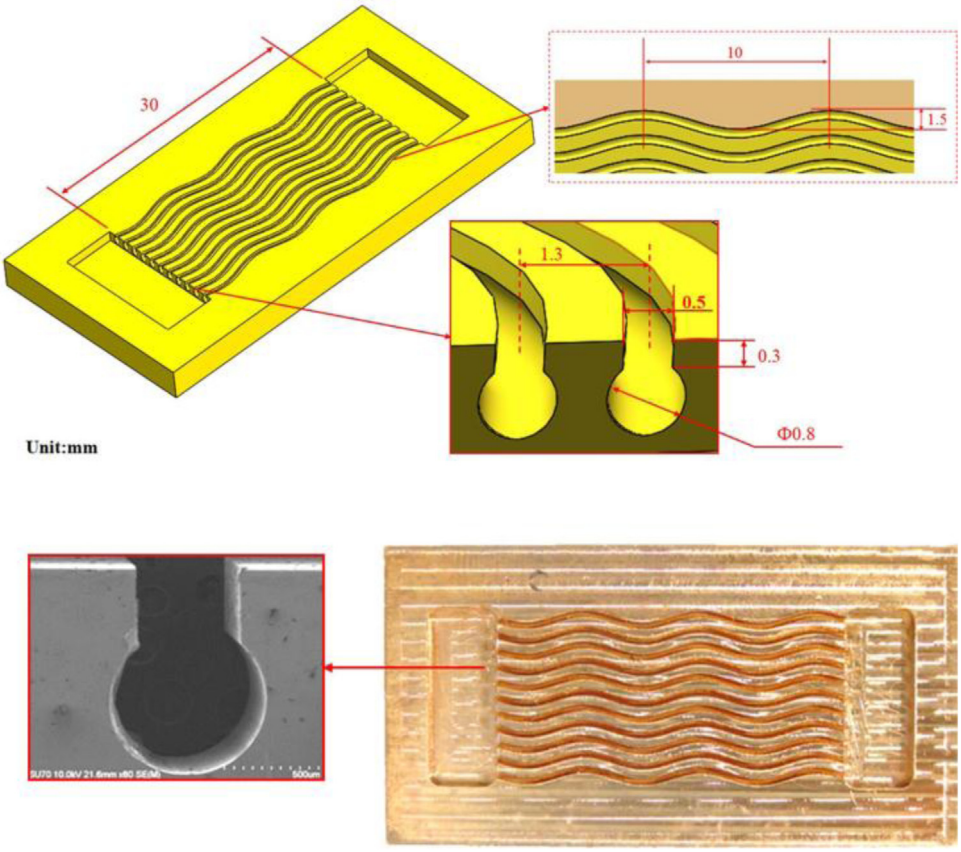

Fig. 16. Serpentine concave MCHS [61].

shown that the addition of grooves mainly promotes the secondary flow of the fluid and enhances the mixing between hot and cold fluids through throttling and jet effects. Among them, the triangular cavity structure and the fan-shaped cavity show the best heat dissipation trend among all cavity structures. However, the cavity structure is difficult to manufacture, and the cost is high. Microchannels with concave cavities have small dimensions and complex structures. Traditional machining methods of turning, milling and drilling make it difficult to manufacture complex concave cavity structures, which can easily cause blockage of the microchannels and reduce the heat transfer performance of the channels. At present, most of the related research is mainly based on simulation.

The above research results all prove that the addition of grooves can reduce the pressure drop loss of MCHS, but this also depends on the shape of the grooves and the magnitude of the Reynolds number, that is, whether the fluid is laminar or turbulent. In the study by Zontul et al. [71] on the flow and heat transfer properties of rectangular grooves at the upper and lower walls in MCHS. The rectangular grooves can indeed enhance the heat transfer but also increase the pressure drop to a certain extent, the possible reason is that the study was carried out in the Re range of $2 \times 10^3 \sim 6.5 \times 10^3$, and the fluid state was turbulent. This is somewhat different from the magnitude of the Re value obtained by Zhu and Pan [67,68] under the conclusion that rectangular grooves improve pressure drop.

2.4.2 Bionic concave cavity structure

The addition of concave cavity structures in the microchannel has been proven to be very effective in improving heat transfer performance. To enhance the heat transfer performance, the combination of concave cavity structures with bionic flow channels has also been designed and analyzed by researchers in recent years. Liu et al. [72] investigated the laminar heat transfer characteristics of the serpentine microchannel by adding fan-shaped concave cavity structures to the microchannel at Re 150–980 (Fig. 18a) and compared the hydraulic characteristics with those of conventional MCHSs. The addition of fan-shaped concave cavities in the serpentine channel not only increases the heat transfer area but also forces the flow to develop jet flows and throttle flows and forms Dean's vortices. This phenomenon effectively inhibits the development of the thermal boundary layer. Shui et al. [73] investigated the addition of concave cavity structures to dendritic branching microchannels to enhance heat transfer (Fig. 18b). The function of the cavity is to ensure flow separation when the fluid passes through the cavity, which can disturb the fluid flow at the wall and weaken the development of the thermal boundary layer. In addition, the effect of dendritic branching is reflected in the higher-level branched flow channels. Due to the reduced diameter of the flow channel, the intensity of the disturbance in the secondary flow can be enhanced, and the heat exchange

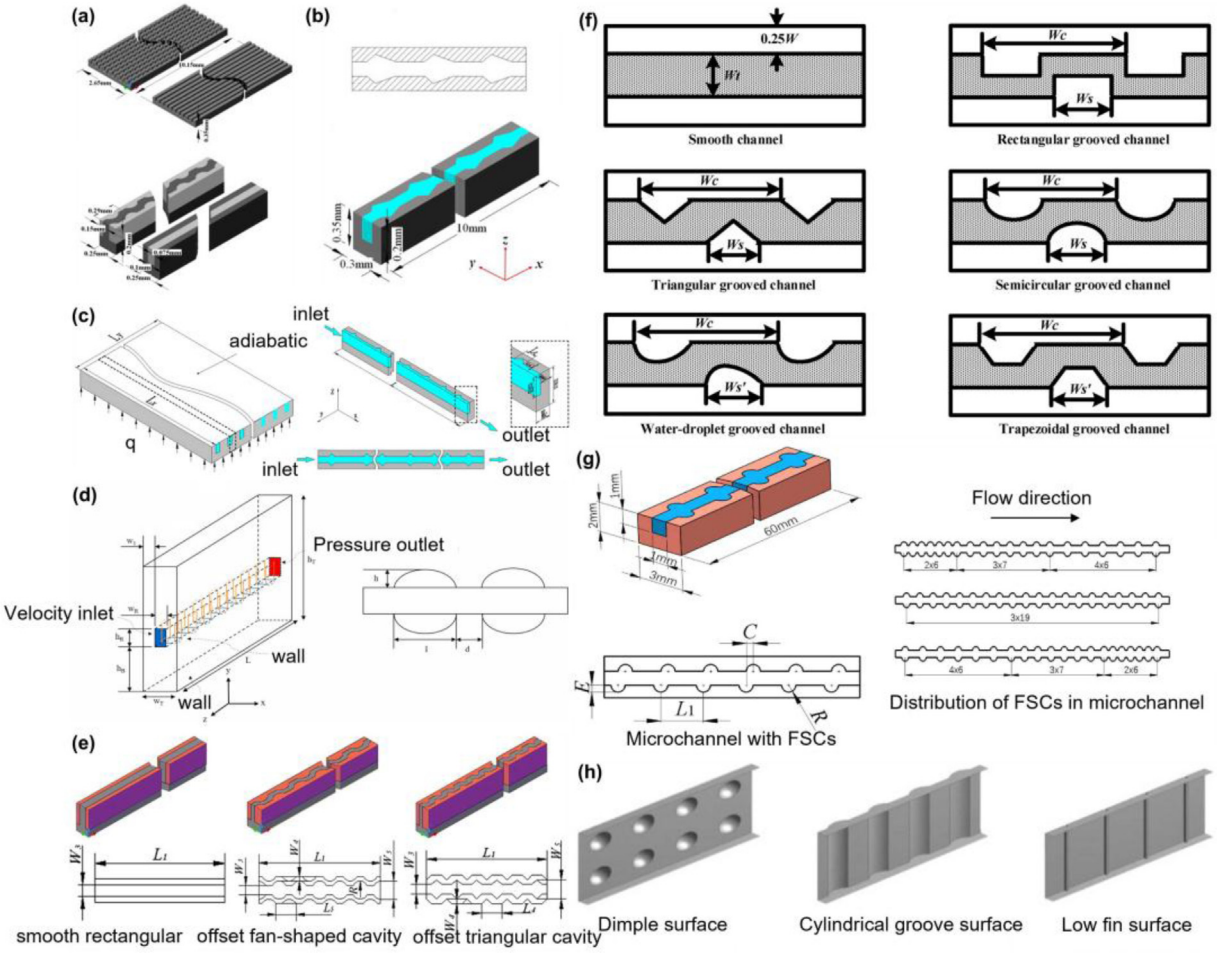

Fig. 17. Different concave cavity structures on the walls (a) Offset fan-shaped concave cavity structure [62] (b) Triangular concave cavity [63] (c) Triangular concave cavity [64] (d) Arc-shaped grooved microchannels [65] (e) Offset fan-shaped cavity structure and offset triangular cavity structure [66] (f) Five different sidewall concave cavity structures [67] (g) Fan-shaped concave cavities with different distribution methods [69] (h) Dimple-shaped, cylindrical grooved and low finned structure [70].

can be further promoted. A similar study was also carried out by Huang et al. [74] for the numerical simulation of the heat transfer and hydraulic performance of dendritic microchannel with rib and concave cavity structures, respectively (Fig. 18c). The dendritic branching structure creates a branching effect and ensures that the fluid flows at a uniform rate in each branch flow channel. Both the concave cavity and the rib structure can cause the interruption and regeneration of the fluid. The concave cavity mixes the hot fluid near the wall with the cold fluid in the center of the channel, while the introduction of ribs promotes the creation of vortices near the ribs and enhances heat transfer performance. Overall, the heat transfer performance of the dendritic microchannel with rib structure is higher than that of the dendritic microchannel with a cavity structure, but the pressure drop loss caused by the rib is significantly higher than that of the cavity. Therefore, the comprehensive evaluation of heat transfer performance and pressure drop loss shows that the tree microfluidic channel with a concave cavity structure has a greater PEC value and offers the best overall performance.

2.5 Hybrid microchannels with reinforced ribs and concave cavities

Adding a structure with the coexistence of ribs and cavities in the microchannel is another method applied to enhance heat transfer. Meanwhile, microchannels with cavity and rib structures have greater advantages in increasing heat transfer area, enhancing fluid disturbance, and improving pressure drop. Yao et al. [75] proposed a MCHS with triangular cavities and ribs to enhance heat transfer performance (Fig. 19a). The combination of the cavity and rib structure effectively prevents the reduction of the Nussle number along the flow direction, which reduces the temperature difference of the optimized MCHS by 9 K. Li et al. [76] proposed four types of MCHS with both cavities and different shaped fins (Fig. 19b). The fins can separate the fluid and enhance the secondary flow strength. At the same time, the cavity can also promote the fluid to take heat away from the solid wall and mix with the cold fluid to enhance heat exchange. Compared to conventional rectangular microchannels, the new microchannels can reduce the thermal resistance by up to 35.3%. However,

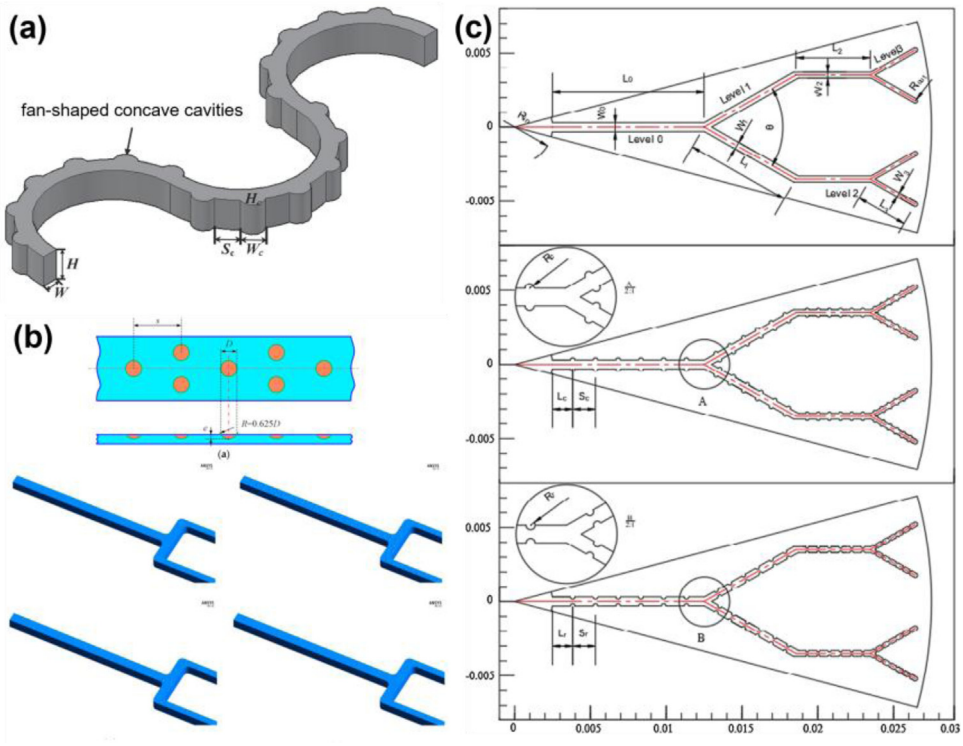

Fig. 18. Bionic concave structured microchannel (a) Serpentine microchannels with fan-shaped concave cavities structure [72] (b) Dendritic branching microchannels with concave cavities structure [73] (c) Dendritic bifurcated microchannels with concave cavities or ribbed structures [74].

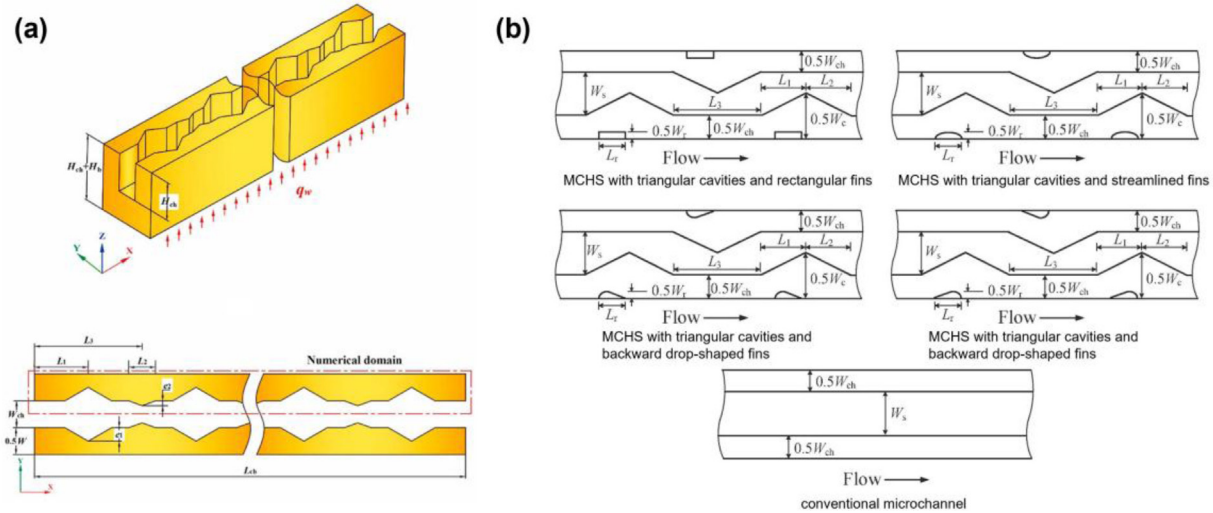

Fig. 19. Microchannels with cavity and rib structures (a) Microchannel with triangular cavity and rib structures [75] (b) MCHS with cavities and different shaped fins [76].

cavities and fins also result in a significant increase in pressure drop. Therefore, the MCHS with isosceles triangular cavities and forward drop-shaped fins shows the best overall performance after a comprehensive analysis of the relationship between thermal resistance and pumping power.

The hybrid structure of cylindrical pin fins and concave cavities has also been shown to have a significant effect on improving heat transfer performance. Feng et al. [77] combined cavities and cylindrical pin fins in the microchannels and compared the heat transfer and hydrodynamic characteristics with conventional smooth linear

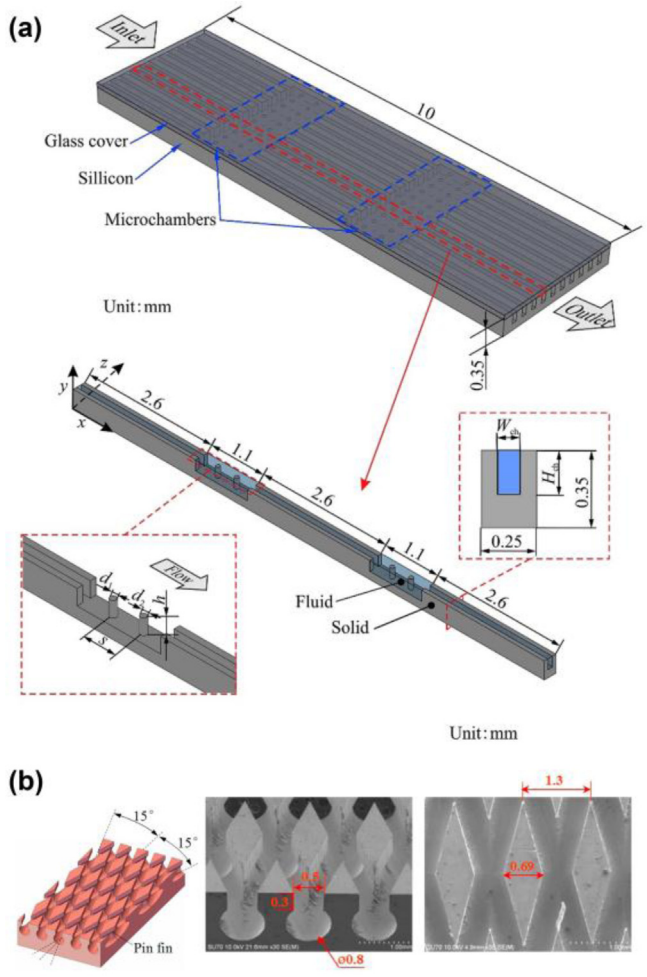

Fig. 20. Microchannel with cavities and ribs (a) Double cylindrical fin concave cavity microchannel [77] (b) Pin fin-interconnected concave cavity microchannel [78].

microchannels and microchannels with only concave cavities (Fig. 20a). The heat transfer performance of the MCHS with concave cavities and cylindrical pin fins is significantly higher than that of the smooth straight and concave cavity microchannels, which is mainly due to the inclusion of pin fins that not only increase the heat transfer area but also promote fluid disturbance in the channels. In particular, the double cylindrical fin microchannel exhibits higher heat transfer performance and better temperature uniformity control due to the larger heat transfer area and more intense flow disturbance which improves the lack of fluid disturbance caused by the single cylindrical fin. Deng et al. [78] proposed a Pin fin-interconnected reentrant microchannel (PFIRM) which combines the structural design of rhombic fin pin fins and concave cavities (Fig. 20b). And its heat transfer and hydraulic characteristics were investigated. The design of the concave cavity provides more space for bubble nucleation, while the diamond-shaped micro-pin fin can divide the slug into two parts due to its protruding tip, which effectively prevents the binding of large bubbles and the creation of long slugs and reduces the bubble confinement effect of microchannels.

3 Geometric design of microchannels in boiling heat transfer

In the boiling heat transfer, the special-shaped cross-section design and the bionic structure design are also used in the structure design of the two-phase microchannel. Walunj and Sathyabhama [79] fabricated rectangular, parabolic and stepped shaped cross-section microchannels on circular copper specimens of 10 mm diameter and compared the effect of flow channel geometry on boiling heat transfer performance (Fig. 21a). The results showed that the heat transfer efficiency of the parabolic and stepped microchannels are increased by 88% and 169% compared to the rectangular microchannels at 11.7 °C wall superheat conditions. This is mainly because the top width of both microchannels is wider than that of the rectangular channel, which is suitable for the growth of bubbles. Li et al. [80] designed a biomimetic microchannel flat heat pipe with a rectangular structured surface based on the strong water-collection and water-transfer capabilities of the Nepenthes surface for use in a fuel cell plate temperature control device (Fig. 21b). The microchannels with rectangular structured surfaces have strong hydraulic transport capacity and the small channel design increases the heat transfer area and circulation efficiency. Compared to conventional flat heat pipes, the thermal resistance is reduced by 22% and the thermal conductivity is increased by more than 40%, which can keep the surface temperature of the fuel cell below 52 °C.

In the boiling heat transfer experiment, the addition of pin-fin fins also has a significant effect on improving the boiling heat transfer coefficient. Deng et al. [81] investigated the enhancement of boiling heat transfer in micro cone pin fins microchannels (Fig. 22a). Compared with the traditional smooth rectangular microchannel, the micro cone pin fins can provide more stable bubble nucleation sites for the microchannel. In general, the structure significantly increases the capillary effect and keeps the walls permanently wetted, which reduces the occurrence of localized drying and increases the critical heat flux. When the fluid medium is water, the microchannel can enhance heat transfer performance by 10–104%. Similar conclusions were also obtained in the two-phase flow experiments of microchannels with micro cylindrical fins studied by Zhu et al. [82], and the micro-column structure can improve the heat transfer effect by 57%. Therefore, adding ribs in the microchannel also provides an effective choice for the heat exchange of the two-phase MCHS. In addition, the different fin shapes have an important influence on the heat transfer characteristics and the hydraulic properties of the microchannels. Wan et al. [83] investigated the flow boiling heat transfer characteristics of MCHS with four different micro pin fin shapes including square, circular, diamond and streamlined fins (Fig. 22b). Since the square surface structure is more conducive to the growth of bubbles and the four vertical sides of the fin can effectively inhibit the continuous development of vapor cores and ensure the long-term wetting of the fin wall, the square fin structure can effectively improve the heat transfer performance of the MCHS. Combined with the current

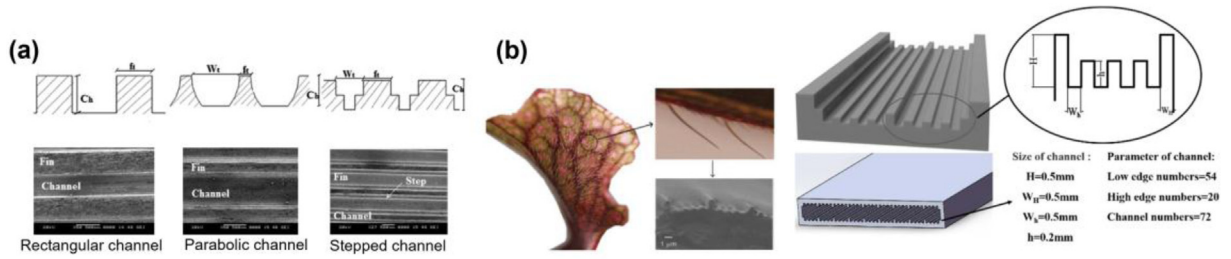

Fig. 21. Microchannels with different cross-sectional shapes (a) Rectangular, parabolic and stepped shaped cross-section microchannels [79] (b) Microchannels imitating the surface structure of Nepenthes [80].

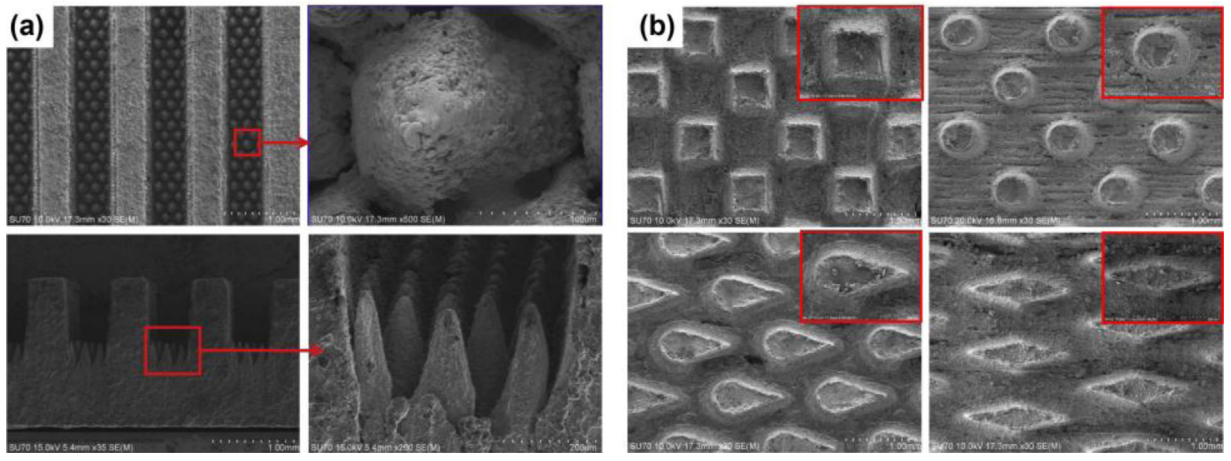

Fig. 22. SEM image of MCHS with pin fins (a) Pin fins on the bottom surface [81] (b) Different pin fin shapes [83].

application of two-phase heat transfer in engineering thermal design, the different fin shapes proposed in this study have important guiding significance for the structural design of flow boiling heat dissipation experiments.

The concave cavity structure in the microchannel also provides good heat transfer enhancement in two-phase boiling heat transfer, which not only increases the capillary effect force in the flow channel but also effectively avoids local drying in the flow channel. Deng et al. [84] investigated the role of porous structures with concave cavities in pool boiling cooling experiments (Fig. 23a). The concave cavity structure can effectively increase the heat transfer area and bubble nucleation density. In addition, the concave cavity can provide a horizontal flow channel for the inflow of the liquid in the boiling experiment, which can effectively prevent the drying of the heat transfer surface and reduce the generation of critical heat flux, with a maximum reduction of 12 °C in surface superheat. Sun et al. [85] showed that the microchannel with concave cavities on the surface has a higher heat transfer coefficient than the smooth copper sheet (Fig. 23b), mainly because the combination of the concave cavities and the microgrooves can increase the capillary force and ensure sufficient fluid replenishment even at high heat flux. At the same time, the cavity structure can also effectively prevent the vapor slugs caused by the binding of bubbles, thus preventing the rapid rise of the wall temperature caused by the separation of the liquid medium from the heating surface. This was similarly concluded in the studies of Zeng and Chen [86,87].

4 MCHS materials and cooling fluid

The structural optimization of the MCHS has a good effect on the improvement of heat transfer performance, but it also inevitably leads to the complication of the processing and the increase in cost. Therefore, the use of high thermal conductivity materials and fluid media is another practical and effective way to solve the problem of high temperature of the devices in recent years. Table 1 summarizes the process methods, solid materials and fluid media used by the above researchers to fabricate the enhanced MCHS.

4.1 MCHS materials

Most of the heat sink materials in Table 1 are single materials whose thermal conductivity cannot fully satisfy the increasing heat flux of electronic devices. Further, composite materials have a higher thermal conductivity than single materials and their lower thermal expansion coefficient can prevent the thermal deformation of the MCHS. Table 2 summarizes the performance indicators of common single materials, alloy materials and diamond/copper composite materials.

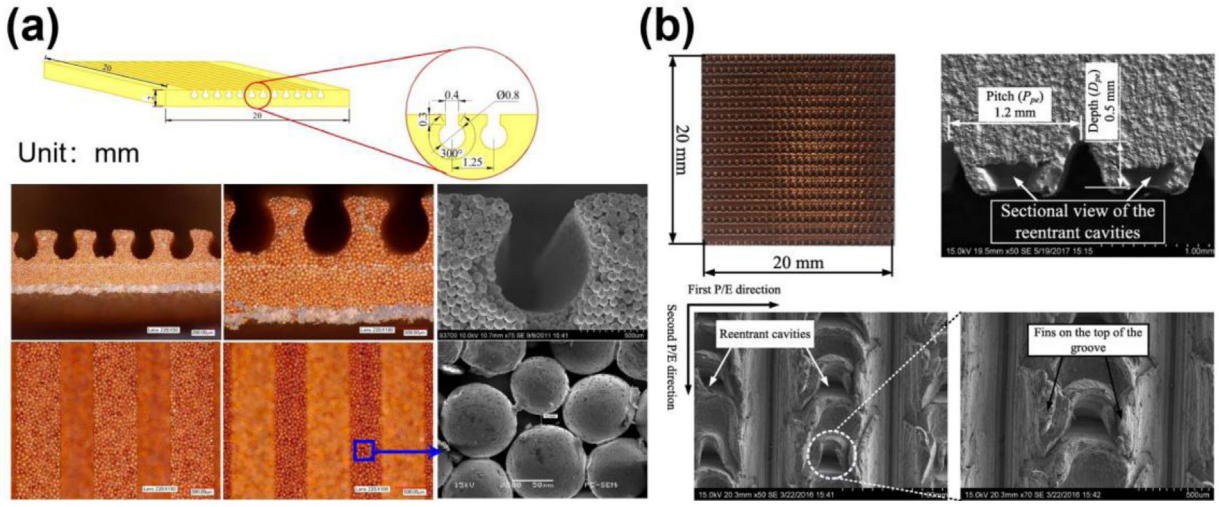

Fig. 23. SEM image of microchannel (a) Porous microchannels with concave cavity structure [84] (b) Microchannels with concave cavities and microgrooves [85].

Diamond/copper matrix composite material has been the most studied in recent years, mainly because it combines the excellent thermal conductivity of diamond and the high working temperature of the copper matrix. The thermal conductivity is three to four times higher than that of conventional thermally conductive materials. Meanwhile, The composite material has a low coefficient of expansion and density that are suitable for integrated devices at the same time, which is one of the best new heat sink materials [88]. Che and Zhao [89,90] prepared diamond/copper composites by spark plasma sintering (SPS). The results show that the thermal conductivity of the two composites is 630 $W \cdot m^{-1} k^{-1}$ and 613 $W \cdot m^{-1} k^{-1}$ when the diamond fraction is 50 vol% and 60 vol%, respectively. Bai et al. [91] prepared Cu-B/diamond composites with a diamond volume fraction of 67 vol% by gas pressure infiltration and studied their high temperature thermal conductivity and thermal expansion coefficient. Finally, the Cu-0.5wt%B/diamond composite was found to have the highest thermal conductivity of 722$W \cdot m^{-1} k^{-1}$. Wu et al. [92] prepared highly thermally conductive copper matrix diamond composites by electrodeposition and introduced two additives (DVF-B and DVF-C) for the first time to synthesize diamond/copper composites. The effect of the additives promoted a good bonding at the diamond/Cu interface. Finally, diamond/copper composites with a tightly bonded interface and an optimum thermal conductivity of 617.87 $W \cdot m^{-1} k^{-1}$ were successfully synthesized. However, few researchers have fabricated diamond/copper matrix composites into practical MCHS. Therefore, diamond/copper composites will be the first choice for fabricating MCHS in subsequent heat dissipation studies.

4.2 Cooling fluid

At present, the most used coolants are water and ethanol. From Table 1, it can be found that the nanofluid as the cooling medium of the MCHS also appeared in the heat exchange experiment. Compared with cooling media such as water and ethanol, nanofluids have higher thermal conductivity, and their nano-sized particles will not cause blockage of the MCHS. However, the presence of particles inevitably results in a certain pressure drop loss. Considering its advantage in improving heat transfer performance, the impact of pressure drop losses is less pronounced. Therefore, nanofluids have broad application prospects in the field of enhancing heat transfer, which is conducive to the development of MCHS toward miniaturization. Li et al. [93] conducted an experimental analysis of the effect of 0.1–0.5 vol% Al_2O_3-nanofluids on the heat transfer performance of microchannels. Compared with deionized water, the nanofluid significantly enhanced the heat transfer performance, and its Nusselt number was 1.12–1.66 times that of deionized water, but the flow resistance was 1.02–1.80 times that of deionized water. In terms of comprehensive performance, nanofluids have a higher PEC value. Wang et al. [94] found that there is an optimum diameter and an optimum volume fraction of nanoparticles to optimize the overall performance of microchannels in convective heat transfer experiments where the medium is a nanofluid. Ali et al. [95] also applied nanofluids to microchannel heat transfer experiments. The results demonstrated that the use of nanofluids instead of conventional coolants significantly improved the overall heat transfer performance of MCHS.

4.3 Manufacturing requirements and challenges

The difficulties in achieving the fabrication of micro- and nano-scale structures in microchannels present a serious challenge for enhanced MCHS. In recent years, microchannels are often manufactured by etching techniques, micromachining, sintering, 3D printing techniques, laser processing techniques, micro discharge processing and vapor phase deposition. Among all the methods, it can be mainly categorized as additive and subtractive materials methods. Etching techniques include wet etching and dry

Table 1. Summary of process methods, solid materials and fluid media used in MCHS.

References	Heat transfer method	Microchannel material	Processing methods	Type of coolant	Years
Perret et al. [7]	Passive	Copper	Wet chemical etching	Water	1998
Wu and Cheng [8]	Passive	Silicon	Wet etching	Deionized water	2003
Chen et al. [9]	Passive	Silicon	Etch	Deionized water	2009
Gunnasegaran et al. [10]	Passive	Aluminum	–	Water	2010
Wang et al. [11]	Passive	Oxygen-free copper	–	Deionized water	2016
Vinoth and Senthil Kumar [12]	Passive	Copper	Wire cut electrical discharge machining	Water and Al2O3/ water nanofluid	2017
Moradikazerouni et al. [13]	Passive	aluminum, alumina (92%), cobalt, stainless steel, copper, and silver	–	Air	2019
Alihosseini et al. [14]	Passive	Copper	–	Water	2021
Hao et al. [15]	Passive	6061 aluminum	–	Water	2014
Al-Neama et al. [16]	Passive	Copper	CNC	Water	2018
Cao et al. [17]	Passive	Copper	EDM	Water	2020
Jaffal et al. [18]	Passive	Copper	CNC	Water	2021
Imran et al. [19]	Passive	Copper	–	Water	2018
Gorzin et al. [20]	Passive	Aluminum alloy	CNC	Water	2022
Peng et al. [21]	Passive	Copper	Wire cutting	Deionized water	2021
Chen and Cheng [22]	Passive	Silicon	Etch	Deionized water	2005
Zhang et al. [23]	Passive	–	–	Water	2011
Fan et al. [25]	Passive	Aluminum		Water	2022
Shui et al. [26]	Passive	Copper	Micro-milling	Steam/air	2018
Ran et al. [27]	Passive	Aluminum	–	Water	2022
Luo et al. [28]	Passive	Copper	Laser engraving and mould coining	Deionized water	2020
Li et al. [29]	Passive	Aluminum	CNC	Deionized water	2019
Peng et al. [31]	Passive	Copper	–	Water	2021
Tan et al. [32]	Passive	6063 aluminum	3D printing technique	Water	2019
Tan et al. [33]	Passive	6063 aluminum alloy	3D printing technique	HFE7200	2021
Han et al. [34]	Passive	Aluminum	3D printing technique	Water	2021
Hu et al. [35]	Passive	Silicon	Etch	Deionized water	2019
Wang et al. [36]	Passive	Aluminum	–	Water	2021
Li et al. [37]	Passive	–	–	Water	2020
Wang et al. [38]	Passive	Copper	CNC	Deionized water	2019

Table 1. (continued).

References	Heat transfer method	Microchannel material	Processing methods	Type of coolant	Years
Zhang et al. [39]	Passive	–	–	Liquid ammonia	2010
Behnampour et al. [40]	Passive	–	–	Nanofluid	2017
Rehman et al. [41]	Passive	Copper	–	Water	2019
Rehman et al. [42]	Passive	Copper	–	Nanofluid	2020
Chai et al. [43–45]	Passive	Silicon	–	Water	2016
Derakhshanpour et al. [46]	Passive	Silicon	–	Water	2020
Adhikari et al. [47]	Passive	anodized Aluminum 6063 −T5 alloy	–	Air	2020
Ben Hamida and Hatami [48]	Passive	Aluminum	–	Al2O3/water nanofluid	2021
Ali et al. [49]	Passive	–	–	Water	2020
Sun et al. [50]	Passive	Copper	–	Water	2022
Zhang et al. [51]	Passive	Aluminum	CNC	Water	2022
Wang et al. [52]	Passive	Silicon	Etch	HFE-7000	2018
Vasilev et al. [53]	Passive	Copper	–	Water	2021
Lyu et al. [54]	Passive	Copper	Sinter	Air	2020
Yan et al. [55]	Passive	Silicon	–	HFE7100	2022
Pan et al. [56]	Passive	Silicon	–	HFE7100	2022
Sreehari and Prajapati [57]	Passive	Copper	–	Water and nanofluid	2021
Jia et al. [58]	Passive	Silicon	–	Deionized water	2018
Zheng et al. [59]	Passive	Copper	UV-LGA	Deionized water	2022
Wang et al. [60]	Passive	Silicon	inductively coupled plasma reactive ion etching	Deionized water	2019
Chen et al. [61]	Passive	Copper	Micro-milling	Water	2022
Chai et al. [62]	Passive	Silicon	–	Water	2011
Xia et al. [63]	Passive	Silicon	–	Water	2011
Li et al. [64]	Passive	Silicon	–	Al2O3-water nanofluid	2019
Kumar and Kumar [65]	Passive	–	–	Water	2021
Xia et al. [66]	Passive	Silicon	–	Deionized water	2015
Zhu et al. [67]	Passive	Silicon	–	Deionized water	2020
Pan et al. [68]	Passive	Copper	–	Water	2019
Pan et al. [69]	Passive	Copper	Micro-milling	Deionized water	2019
Bi et al. [70]	Passive	–	–	Water	2013
Zontul et al. [71]	Passive	6061 aluminum	–	Water	2021
Liu et al. [72]	Passive	–	–	Water	2019
Shui et al. [73]	Passive	Copper	Micro-milling	Air	2018
Huang et al. [74]	Passive	Copper	–	Water	2020
Yao et al. [75]	Passive	Silicon	–	Water	2021
Li et al. [76]	Passive	Silicon	–	Deionized water	2020
Feng et al. [77]	Passive	Silicon	–	Water	2021

Table 1. (continued).

References	Heat transfer method	Microchannel material	Processing methods	Type of coolant	Years
Deng et al. [78]	Passive	Copper	Micro-milling	Deionized water and ethanol	2019
Walunj and Sathyabhama [79]	Passive	Copper	Wire edm	Deionized water	2018
Li et al. [80]	Passive	Copper	Laser etching	Deionized water	2022
Deng et al. [81]	Passive	cooper (99.9% Cu)	micro wire electrical discharge machining	Deionized water and ethanol	2017
Zhu et al. [82]	Passive	Silicon	Etch	Degassed and high purity water	2016
Wan et al. [83]	Passive	Copper	Laser micro-milling	Deionized water	2017
Deng et al. [84]	Passive	Copper	solid-state sintering	water and ethanol	2016
Sun et al. [85]	Passive	Pure copper	orthogonal Ploughing/ Extrusion (P/E)	Deionized water	2017
Zeng et al. [86]	Passive	Copper	orthogonal Ploughing/ Extrusion	Deionized water	2017
Chen et al. [87]	Passive	Copper	Orthogonal Ploughing/ Extrusion	Deionized water	2020

Table 2. Summary of performance indicators for common thermal conductive materials.

Material	Coefficient of thermal expansion ($10^{-6}K^{-1}$)	Coefficient of thermal conductivity ($W\,m^{-1}\,K^{-1}$)	Density ($g\,cm^{-3}$)
Cu	17.2	400	8.92
Al	23.6	238	2.70
Si	4.2	151	2.30
Al/Si	7–17	75–180	2.4–2.5
Cu/W	6.5–8.5	140–210	15.65–17.0
CuMo	6.5–8.5	150–200	9.7–10.0
Al_2O_3	6.7	17	3.60
BeO	7.6	250	2.90
SiC/Al	7.3	175	3.03
SiC/Cu	7–11	280–360	7–9
Diamond/Al	7–9	350–750	3.0
Diamond/Cu	4–8	400–930	5.0

etching, which can manufacture more complex microchannel structures including some flow distribution structures. However, etching techniques are time consuming and often associated with toxic chemical solutions, which should also be considered when preparing microchannels. Micromachining can machine metal materials such as steel, aluminum and copper. This method does not require expensive equipment or machining technology. However, the preparation of microchannels is prone to cutting burrs and tool wear, reducing the quality of the cut. The sintering technique is commonly used to prepare porous media for microchannel boiling heat transfer. The method has low production costs and is expected to be used for industrial applications. 3D printing is one of the most typical additive manufacturing technologies. In the preparation of microchannels, material losses can be reduced, and the process is simple. However, current 3D printing techniques have poor geometric accuracy and surface flatness of the channel surface when manufacturing channels on the micron scale. Laser processing technology has high preparation

accuracy, which allows the processing of various complex microchannel structures such as concave cavities and pin fins. However, laser processing equipment is expensive, and the processing time is long. The high heat concentration generated by the laser can also lead to oxidation of the material and cause the poor surface finish of the channels. The low productivity of micro discharge machining and vapor deposition makes it difficult to achieve mass production. In conclusion, the relationship between machining accuracy and machining cost should be considered simultaneously when machining microchannels.

5 Conclusion and outlook

This paper reviews the progress of research on the optimal design of channel geometry for MCHS under the experimental conditions of single-phase flow heat transfer and two-phase boiling heat transfer for high heat flux electronic devices. In addition, the selection of materials and fluid media for MCHS in recent years is reviewed. The optimized design of channel geometry includes a special-shaped cross-section channel design, topological biomimetic channel design, and rib and cavity structure design in the fluid interruption structure. The following conclusions can be drawn from different structural optimization designs:

- The influence of the special-shaped cross-sections on the heat transfer performance of MCHS is mainly reflected in the difference in the actual heat transfer area of the microchannel and the existence of the flow dead zone. Among all the investigated microchannels, the triangular and trapezoidal cross-section microchannels tend to exhibit better heat transfer characteristics.
- Topologically optimized microchannels are gradually developing from the traditional serpentine microchannels to biomimetic channels with wider distribution areas, such as tree-shaped, leaf-vein shaped and spider-web shaped structures. The presence of bends in the serpentine channels, the branching and merging characteristics of the dendritic and vein-shaped microchannels and the large heat transfer area of the spider-web shaped channels are the main reasons for the enhanced heat transfer performance of these topological biomimetic microchannels. In addition, the topologically biomimetic optimized microchannel design shows outstanding advantages in temperature uniformity control. In all above biomimetic MCHS studies, the temperature difference can be controlled within 2 °C.
- Microchannels with rib structures enhance heat transfer by interrupting the fluid flow and enhancing fluid turbulence. The rib structures are mainly divided into sidewall rib structures, staggered rib structures and cylindrical pin fin structures. Different rib microchannel structures and their geometric parameters have different effects on their heat transfer performance and hydraulic properties. Among all the sidewall rib microchannels, the triangular sidewall rib microchannel is proven to have better heat transfer performance. However, the staggered rib structures and the cylindrical pin fin structures show better heat transfer characteristics than the sidewall rib structures. In summary, microchannels with ribs can significantly improve heat transfer performance by around 50% compared to conventional smooth rectangular channels.
- The function of the concave cavity microchannels is similar to that of the ribbed microchannels, which also enhance heat transfer by interrupting the fluid and promoting fluid perturbation. However, the difference is that the concave cavity microchannels suppress the development of thermal boundary layers mainly through throttling and jet effects. Among the sidewall concave cavity structures, the triangular concave cavity currently exhibits better heat transfer characteristics with the highest Nussle number. The biomimetic microchannels with concave cavity structures combine the advantages of topological bionics to improve heat transfer.
- The current research on microfluidics mainly focuses on numerical simulation analysis mainly because of the difficulty and high manufacturing cost of complex structures such as ribs and cavities. In future practical engineering applications, overcoming manufacturing difficulties and reducing processing costs are the primary tasks. Secondly, the research on the structure of the MCHS needs to be more comprehensive and systematic.

The heat sink materials studied mainly focus on copper and silicon in recent years, and diamond/copper composite materials will become the first choice for the MCHS due to their high thermal conductivity and low expansion coefficient. In addition, the existence of nanoparticles in the nanofluid can significantly improve the heat transfer capacity, which has a very prominent application prospect in the future heat transfer experiments of MCHS.

Declaration of competing interest

The authors declare that there are no known competing financial interests or personal relationships that could have appeared to influence the work reported in this paper.

Funding Information

State Administration of Science, Technology and Industry for National Defense (No. JCKY2020203B056), Natural Science Foundation of Jiangsu Province (No. BK2022010), the Natural Science Foundation of Jiangsu Higher Education Institution of China (No. 20KJA460003), the National Natural Science Foundation of China (No. 52075250), Shanghai Aerospace Science and Technology Innovation Fund (No. SAST2021-064), Six Talent Peaks in Jiangsu Province (GDZB-069).

References

1. L. Gong, J. Zhao, S.B. Huang, Numerical study on layout of micro-channel heat sink for thermal management of electronic devices, Appl. Therm. Eng. **88** (2015) 480–490
2. J.R. Black, Electromigration – a brief survey and some recent results, IEEE Trans. Electron Dev. Ed. **16** (1969) 338

3. A. Sommers, Q. Wang, X. Han, T'C. Joen, Y. Park, A. Jacobi, Ceramics and ceramic matrix composites for heat exchangers in advanced thermal systems − a review, Appl. Therm. Eng. **30** (2010) 1277–1291
4. D.B. Tuckerman, R.F.W. Pease, High-performance heat sinking for VLSI, Electr. Device Lett. **2** (1981) 126–129
5. P. Smakulski, S. Pietrowicz, A review of the capabilities of high heat flux removal by porous materials, microchannels and spray cooling techniques, Appl. Therm. Eng. **104** (2016) 636–646
6. Y.L. Zhai, G.D. Xia, X.F. Liu, Y.F. Li, Exergy analysis and performance evaluation of flow and heat transfer in different micro heat sinks with complex structure, Int. J. Heat Mass Transfer **84** (2015) 293–303
7. C. Perret, C. Schaeffer, J. Boussey, Microchannel integrated heat sinks in silicon technology, in *Industry Applications Conference. Thirty-Third IAS Annual Meeting*. The 1998 IEEE (1998)
8. H.Y. Wu, P. Cheng, An experimental study of convective heat transfer in silicon microchannels with different surface conditions, Int. J. Heat Mass Transfer **46** (2003) 2547–2556
9. Y.P. Chen, C.B. Zhang, M.H. Shi, J.F. Wu, Three-dimensional numerical simulation of heat and fluid flow in noncircular microchannel heat sinks, Int. Commun. Heat Mass Transfer **36** (2009) 917–920
10. P. Gunnasegaran, H.A. Mohammed, N.H. Shuaib, R. Saidur, The effect of geometrical parameters on heat transfer characteristics of microchannels heat sink with different shapes, Int. Commun. Heat Mass Transfer **37** (2010) 1078–1086
11. H. Wang, Z. Chen, J. Gao, Influence of geometric parameters on flow and heat transfer performance of micro-channel heat sinks, Appl. Therm. Eng. **107** (2016) 870–879
12. R. Vinoth, S.D. Kumar, Channel cross section effect on heat transfer performance of oblique finned microchannel heat sink, Int. Commun. Heat Mass Transfer **87** (2017) 270–276
13. A. Moradikazerouni, M. Afrand, J. Alsarraf, O. Mahian, S. Wongwises, M.-D. Tran, Comparison of the effect of five different entrance channel shapes of a micro-channel heat sink in forced convection with application to cooling a supercomputer circuit board, Appl. Therm. Eng. **150** (2019) 1078–1089
14. Y. Alihosseini, M.R. Azaddel, S. Moslemi, M. Mohammadi, A. Pormohammad, M.Z. Targhi, M.M. Heyhat, Effect of liquid cooling on PCR performance with the parametric study of cross-section shapes of microchannels, Sci. Rep. **11** (2021) 16072
15. X. Hao, B. Peng, G. Xie, Y. Chen, Thermal analysis and experimental validation of laminar heat transfer and pressure drop in serpentine channel heat sinks for electronic cooling, J. Electr. Packag. **136** (2014) 031009
16. A.F. Al-Neama, N. Kapur, J. Summers, H.M. Thompson, Thermal management of GaN HEMT devices using serpentine minichannel heat sinks, Appl. Therm. Eng. **140** (2018) 622–636
17. X. Cao, H.L. Liu, X.D. Shao, H. Shen, G.N. Xie, Thermal performance of double serpentine minichannel heat sinks: effects of inlet-outlet arrangements and through-holes, Int. J. Heat Mass Transfer **153** (2020)
18. H.M. Jaffal, B. Freegah, A.A. Hussain, A. Hasan, Effect of the fluid flow fragmentation on the hydrothermal performance enhancement of a serpentine mini-channel heat sink, Case Stud. Thermal Eng. **24** (2021) 100866
19. A.A. Imran, N.S. Mahmoud, H.M. Jaffal, Numerical and experimental investigation of heat transfer in liquid cooling serpentine mini-channel heat sink with different new configuration models, Therm. Sci. Eng. Progr. **6** (2018) 128–139
20. M. Gorzin, A.A. Ranjbar, M.J. Hosseini, Experimental and numerical investigation on thermal and hydraulic performance of novel serpentine minichannel heat sink for liquid CPU cooling, Energy Rep. **8** (2022) 3375–3385
21. Y. Peng, Z.B. Li, S.B. Li, B. Cao, X. Wu, X.F. Zhao, The experimental study of the heat ransfer performance of a zigzag-serpentine microchannel heat sink, Int. J. Thermal Sci. **163** (2021) 106831
22. Y.P. Chen, P. Cheng, An experimental investigation on the thermal efficiency of fractal tree-like microchannel nets, Int. Commun. Heat Mass Transfer **32** (2005) 931–938
23. C. Zhang, Y. Chen, R. Wu, M. Shi, Flow boiling in constructal tree-shaped minichannel network, Int. J. Heat Mass Transfer **54** (2011) 202–209
24. Y.W. Fan, Z.H. Wang, T. Fu, Multi-objective optimization design of lithium-ion battery liquid cooling plate with double-layered dendritic channels, Appl. Therm. Eng. **199** (2021) 117541
25. Y.W. Fan, Z.H. Wang, T. Fu, H.W. Wu, Numerical investigation on lithium-ion battery thermal management utilizing a novel tree-like channel liquid cooling plate exchanger, Int. J. Heat Mass Transfer **183** (2022) 122143
26. L.Q. Shui, B. Huang, F. Gao, H.B. Rui, Experimental and numerical investigation on the flow and heat transfer characteristics in a tree-like branching microchannel, J. Mech. Sci. Technol. **32** (2018) 937–946
27. Y. Ran, Y.F. Su, L. Chen, K. Yan, C.X. Yang, Y. Zhao, Investigation on thermal performance of water-cooled Li-ion cell and module with tree-shaped channel cold plate, J. Energy Storage **50** (2022) 104040
28. Y. Luo, W. Liu, G. Huang, Fabrication and experimental investigation of the bionic vapor chamber, Appl. Therm. Eng. **168** (2020) 114889
29. H. Li, X.H. Ding, D.L. Jing, M. Xiong, F.Z. Meng, Experimental and numerical investigation of liquid-cooled heat sinks designed by topology optimization, Int. J. Thermal Sci. **146** (2019) 106065
30. H. Tan, K. Zong, P. Du, Temperature uniformity in convective leaf vein-shaped fluid microchannels for phased array antenna cooling, Int. J. Thermal Sci. **150** (2020) 106224
31. Y. Peng, X. Yang, Z.B. Li, S.B. Li, B. Cao, Numerical simulation of cooling performance of heat sink designed based on symmetric and asymmetric leaf veins, Int. J. Heat Mass Transfer **166** (2021) 120721
32. H. Tan, L. Wu, M. Wang, Z. Yang, P. Du, Heat transfer improvement in microchannel heat sink by topology design and optimization for high heat flux chip cooling, Int. J. Heat Mass Transfer **129** (2019) 681–689
33. H. Tan, P. Du, K. Zong, G. Meng, X. Gao, Y. Li, Investigation on the temperature distribution in the two-phase spider netted microchannel network heat sink with non-uniform heat flux, Int. J. Thermal Sci. **169** (2021) 107079
34. X.-h. Han, H.-l. Liu, G. Xie, L. Sang, J. Zhou, Topology optimization for spider web heat sinks for electronic cooling, Appl. Therm. Eng. **195** (2021) 117154
35. D.H. Hu, Z.W. Zhang, Q. Li, Numerical study on flow and heat transfer characteristics of microchannel designed using topological optimizations method, Sci. China Technol. Sci. **63** (2020) 105–115

36. Z. Wang, B. Li, Q.-Q. Luo, W. Zhao, Effect of wall roughness by the bionic structure of dragonfly wing on microfluid flow and heat transfer characteristics, Int. J. Heat Mass Transfer **173** (2021) 121201
37. P. Li, D. Guo, X. Huang, Heat transfer enhancement, entropy generation and temperature uniformity analyses of shark-skin bionic modified microchannel heat sink, Int. J. Heat Mass Transfer **146** (2020) 118846
38. X.W. Wang, Z.P. Wan, Q.H. Lin, Y. Tang, Study on the flow and heat transfer characteristics of sinusoidal half-corrugated microchannels, J. Thermophys. Heat Transfer **34** (2020) 314–321
39. C. Zhang, Y. Chen, M. Shi, Effects of roughness elements on laminar flow and heat transfer in microchannels, Chem. Eng. Process. **49** (2010) 1188–1192
40. A. Behnampour, O.A. Akbari, M.R. Safaei, M. Ghavami, A. Marzban, Sheikh G.A. Shabani, M. Zarringhalam, R. Mashayekhi, Analysis of heat transfer and nanofluid fluid flow in microchannels with trapezoidal, rectangular and triangular shaped ribs, Physica E **91** (2017) 15–31
41. M.M.U. Rehman, T.A. Cheema, F. Ahmad, M. Khan, A. Abbas, Thermodynamic assessment of microchannel heat sinks with novel sidewall ribs, J. Thermophys. Heat Transfer **34** (2020) 243–254
42. M.M.U. Rehman, T.A. Cheema, M. Khan, A. Abbas, H. Ali, C.W. Park, Parametric evaluation of a hydrofoil-shaped sidewall rib-employed microchannel heat sink with and without nano-encapsulated phase change material slurry as coolant, Appl. Therm. Eng. **178** (2020) 115514
43. L. Chai, G.D. Xia, H.S. Wang, Parametric study on thermal and hydraulic characteristics of laminar flow in microchannel heat sink with fan-shaped ribs on sidewalls − Part 1: Heat transfer, Int. J. Heat Mass Transfer **97** (2016) 1069–1080
44. L. Chai, G.D. Xia, H.S. Wang, Parametric study on thermal and hydraulic characteristics of laminar flow in microchannel heat sink with fan-shaped ribs on sidewalls − Part 2: Pressure drop, Int. J. Heat Mass Transfer **97** (2016) 1081–1090
45. L. Chai, G.D. Xia, H.S. Wang, Parametric study on thermal and hydraulic characteristics of laminar flow in microchannel heat sink with fan-shaped ribs on sidewalls − Part 3: Performance evaluation, Int. J. Heat Mass Transfer **97** (2016) 1091–1101
46. K. Derakhshanpour, R. Kamali, M. Eslami, Effect of rib shape and fillet radius on thermal-hydrodynamic performance of microchannel heat sinks: a CFD study, Int. Commun. Heat Mass Transfer **119** (2020) 104928
47. R.C. Adhikari, D.H. Wood, M. Pahlevani, An experimental and numerical study of forced convection heat transfer from rectangular fins at low Reynolds numbers, Int. J. Heat Mass Transfer **163** (2020) 120418
48. M.B. Ben Hamida, M. Hatami, Optimization of fins arrangements for the square light emitting diode (LED) cooling through nanofluid-filled microchannel, Sci. Rep. UK **11** (2021) 12610
49. E. Ali, J. Park, H. Park, Numerical investigation of enhanced heat transfer in a rectangular channel with winglets, Heat Transfer Eng. **42** (2020) 695–705
50. L. Sun, J. Li, H. Xu, J. Ma, H. Peng, Numerical study on heat transfer and flow characteristics of novel microchannel heat sinks, Int. J. Thermal Sci. **176** (2022) 107535
51. F. Zhang, B. Wu, B. Du, Heat transfer optimization based on finned microchannel heat sink, Int. J. Thermal Sci. **172** (2022) 107357
52. Y.Y. Wang, J.H. Shin, C. Woodcock, X.F. Yu, Y. Peles, Experimental and numerical study about local heat transfer in a microchannel with a pin fin, Int. J. Heat Mass Transfer **121** (2018) 534–546
53. M.P. Vasilev, R.S. Abiev, R. Kumar, Effect of circular pin-fins geometry and their arrangement on heat transfer performance for laminar flow in microchannel heat sink, Int. J. Thermal Sci. **170** (2021) 107177
54. Y.S. Lyu, H.Y. Yu, Y.H. Hu, Q.L. Shu, J. Wang, Bionic design for the heat sink inspired by phyllotactic pattern, Proc. Inst. Mech. Eng. C **235** (2021) 3087–3094
55. Y. Yan, D. Wang, F. Xu, Z. He, Z. Yang, Numerical study on hot spots thermal management in low pressure gradient distribution narrow microchannel embedded with pin fins, Int. J. Heat Mass Transfer **186** (2022) 122518
56. Y.H. Pan, R. Zhao, Y.L. Nian, W.L. Cheng, Study on the flow and heat transfer characteristics of pin-fin manifold microchannel heat sink, Int. J. Heat Mass Transfer **183** (2022) 122052
57. D. Sreehari, Y.K. Prajapati, Comparative analysis of heat transfer and fluid flow in circular and rhombus pin fin heat sink using nanofluid, J. Thermal Sci. Eng. Appl. **13** (2021) 051028
58. Y. Jia, G. Xia, Y. Li, D. Ma, B. Cai, Heat transfer and fluid flow characteristics of combined microchannel with cone-shaped micro pin fins, Int. Commun. Heat Mass Transfer **92** (2018) 78–89
59. R. Zheng, Y.J. Wu, Y.H. Li, G.L. Wang, G.F. Ding, Y.N. Sun, Development of a hierarchical microchannel heat sink with flow field reconstruction and low thermal resistance for high heat flux dissipation, Int. J. Heat Mass Transfer **182** (2022) 121925
60. G. Wang, N. Qian, G. Ding, Heat transfer enhancement in microchannel heat sink with bidirectional rib, Int. J. Heat Mass Transfer **136** (2019) 597–609
61. L. Chen, D.X. Deng, Q.X. Ma, Y.X. Yao, X.H. Xu, Performance evaluation of high concentration photovoltaic cells cooled by microchannels heat sink with serpentine reentrant microchannels, Appl. Energy **309** (2022) 118478
62. L. Chai, G. Xia, M. Zhou, J. Li, Numerical simulation of fluid flow and heat transfer in a microchannel heat sink with offset fan-shaped reentrant cavities in sidewall, Int. Commun. Heat Mass Transfer **38** (2011) 577–584
63. G. Xia, L. Chai, H. Wang, M. Zhou, Z. Cui, Optimum thermal design of microchannel heat sink with triangular reentrant cavities, Appl. Therm. Eng. **31** (2011) 1208–1219
64. F. Li, W. Zhu, H. He, Field synergy analysis on flow and heat transfer characteristics of nanofluid in microchannel with non-uniform cavities configuration, Int. J. Heat Mass Transfer **144** (2019) 118617
65. K. Kumar, P. Kumar, Effect of groove depth on hydrothermal characteristics of the rectangular microchannel heat sink, Int. J. Thermal Sci. **161** (2021) 106730
66. G.D. Xia, J. Jiang, J. Wang, Y.L. Zhai, D.D. Ma, Effects of different geometric structures on fluid flow and heat transfer performance in microchannel heat sinks, Int. J. Heat Mass Transfer **80** (2015) 439–447
67. Q.F. Zhu, H.X. Xia, J.J. Chen, X.M. Zhang, K.P. Chang, H.W. Zhang, H. Wang, J.F. Wan, Y.Y. Jin, Fluid flow and heat transfer characteristics of microchannel heat sinks with different groove shapes, Int. J. Thermal Sci. **161** (2021) 106721

68. M.Q. Pan, H.Q. Wang, Y.J. Zhong, T.Y. Fang, X.E. Zhong, Numerical simulation of the fluid flow and heat transfer characteristics of microchannel heat exchangers with different reentrant cavities, Int. J. Numer. Methods Heat Fluid Flow **29** (2019) 4334–4348
69. M.Q. Pan, H.Q. Wang, Y.J. Zhong, M.L. Hu, X.Y. Zhou, G.P. Dong, P.N. Huang, Experimental investigation of the heat transfer performance of microchannel heat exchangers with fan-shaped cavities, Int. J. Heat Mass Transfer **134** (2019) 1199–1208
70. C. Bi, G.H. Tang, W.Q. Tao, Heat transfer enhancement in mini-channel heat sinks with dimples and cylindrical grooves, Appl. Therm. Eng. **55** (2013) 121–132
71. H. Zontul, H. Hamzah, N. Kurtulmus, B. Sahin, Investigation of convective heat transfer and flow hydrodynamics in rectangular grooved channels, Int. Commun. Heat Mass Transfer **126** (2021) 105366
72. X. Liu, H. Zhang, C. Zhu, F. Wang, Z. Li, Effects of structural parameters on fluid flow and heat transfer in a serpentine microchannel with fan-shaped reentrant cavities, Appl. Therm. Eng. **151** (2019) 406–416
73. L.Q. Shui, J.H. Sun, F. Gao, C.Y. Zhang, Flow and heat transfer in the tree-like branching microchannel with/without dimples, Entropy-Switz **20** (2018) 379
74. P.N. Huang, G.P. Dong, X.N. Zhong, M.Q. Pan, Numerical investigation of the fluid flow and heat transfer characteristics of tree-shaped microchannel heat sink with variable cross-section, Chem. Eng. Process **147** (2020) 107769
75. P. Yao, Y. Zhai, Z. Li, X. Shen, H. Wang, Thermal performance analysis of multi-objective optimized microchannels with triangular cavity and rib based on field synergy principle, Case Stud. Thermal Eng. **25** (2021) 100963
76. Y. Li, Z. Wang, J. Yang, H. Liu, Thermal and hydraulic characteristics of microchannel heat sinks with cavities and fins based on field synergy and thermodynamic analysis, Appl. Therm. Eng. **175** (2020) 115348.
77. Z. Feng, Z. Hu, Y. Lan, Z. Huang, J. Zhang, Effects of geometric parameters of circular pin-fins on fluid flow and heat transfer in an interrupted microchannel heat sink, Int. J. Thermal Sci. **165** (2021) 106956
78. D.X. Deng, L. Chen, W. Wan, T. Fu, X. Huang, Flow boiling performance in pin fin- interconnected reentrant microchannels heat sink in different operational conditions, Appl. Therm. Eng. **150** (2019) 1260–1272
79. A. Walunj, A. Sathyabhama, Comparative study of pool boiling heat transfer from various microchannel geometries, Appl. Therm. Eng. **128** (2018) 672–683
80. H.W. Li, J. Ren, D.D. Yin, G.L. Lu, C.H. Du, X. Jin, Y.T. Jia, Effects of inclination angle and heat power on heat transfer behavior of flat heat pipe with bionic grading microchannels, Appl. Therm. Eng. **206** (2022) 118079
81. D. Deng, W. Wan, Y. Qin, J. Zhang, X. Chu, Flow boiling enhancement of structured microchannels with micro pin fins, Int. J. Heat Mass Transfer **105** (2017) 338–349
82. Y. Zhu, D.S. Antao, K.-H. Chu, S. Chen, T.J. Hendricks, T. Zhang, E.N. Wang, Surface structure enhanced microchannel flow boiling, J. Heat Transfer **138** (2016) 091501
83. W. Wan, D. Deng, Q. Huang, T. Zeng, Y. Huang, Experimental study and optimization of pin fin shapes in flow boiling of micro pin fin heat sinks, Appl. Therm. Eng. **114** (2017) 436–449
84. D. Deng, J. Feng, Q. Huang, Y. Tang, Y. Lian, Pool boiling heat transfer of porous structures with reentrant cavities, Int. J. Heat Mass Transfer **99** (2016) 556–568
85. Y. Sun, G. Chen, S. Zhang, Y. Tang, J. Zeng, W. Yuan, Pool boiling performance and bubble dynamics on microgrooved surfaces with reentrant cavities, Appl. Therm. Eng. **125** (2017) 432–442
86. J. Zeng, S. Zhang, Y. Tang, Y. Sun, W. Yuan, Flow boiling characteristics of micro-grooved channels with reentrant cavity array at different operational conditions, Int. J. Heat Mass Transfer **114** (2017) 1001–1012
87. G. Chen, M. Jia, S. Zhang, Y. Tang, Z. Wan, Pool boiling enhancement of novel interconnected microchannels with reentrant cavities for high-power electronics cooling, Int. J. Heat Mass Transfer **156** (2020) 119836
88. R. Liu, G. Luo, Y. Li, J. Zhang, Q. Shen, L. Zhang, Microstructure and thermal properties of diamond/copper composites with Mo2C in-situ nano-coating, Surf. Coat. Technol. **360** (2019) 376–381
89. Q.L. Che, J.J. Zhang, X.K. Chen, Y.Q. Ji, Y.W. Li, L.X. Wang, S.Z. Cao, L. Guo, Z. Wang, S.W. Wang, Z.K. Zhang, Y.G. Jiang, Spark plasma sintering of titanium-coated diamond and copper-titanium powder to enhance thermal conductivity of diamond/copper composites, Mater. Sci. Semiconductor Process. **33** (2015) 67–75
90. D. Zhao, S. Zha, D. Liu, Influence of sputtering and electroless plating of Cr/Cu dual-layer structure on thermal conductivity of diamond/copper composites, Diamond Relat. Mater. **115** (2021) 108296
91. G.Z. Bai, Y.J. Zhang, X.Y. Liu, J.J. Dai, X.T. Wang, H.L. Zhang, High-temperature thermal conductivity and thermal cycling behavior of Cu-B/diamond composites, IEEE Trans. Comp. Pack Manag. **10** (2020) 626–636
92. Y. Wu, Z. Tang, Y. Wang, P. Cheng, H. Wang, G. Ding, High thermal conductive Cu-diamond composites synthesized by electrodeposition and the critical effects of additives on void-free composites, Ceram. Int. **45** (2019) 19658–19668
93. C.Q. Li, J. Huang, Y.L. Shang, H.Y. Huang, Study on the flow and heat dissipation of water-based alumina nanofluids in microchannels, Case Stud. Thermal Eng. **22** (2020) 100746
94. J. Wang, K. Yu, M.Z. Ye, E. Wang, W. Wang, B. Sunden, Effects of pin fins and vortex generators on thermal performance in a microchannel with Al_2O_3 nanofluids, Energy **239** (2022) 122606
95. A.M. Ali, M. Angelino, A. Rona, Numerical analysis on the thermal performance of microchannel heat sinks with Al_2O_3 nanofluid and various fins, Appl. Therm. Eng. **198** (2021) 117458

Cite this article as: Kaijie Lu, Chunju Wang, Changrui Wang, Xueliang Fan, Fei Qi, Haidong He, Topological structures for microchannel heat sink applications – a review, Manufacturing Rev. **10**, 2 (2023)